

Responses to comments by Reviewer #1

We thank Dr. Du's careful consideration of our work. In this rebuttal, we have addressed all the comments formulated by the Reviewer by replying (in black) to his remarks (in blue). The lines numbers in this rebuttal refer to the revised version of the manuscript.

General comments:

The article used an analytical tidal model to understand the change of freshwater discharge on the tidal dynamics in the Yangtze River, with a specific focus on the impact of Three Gorge Dam. While freshwater discharge's effect on tidal dynamics is well recognized by observations and numerical models, it is rare to use an analytical tool to understand the underlying mechanism (e.g., bottom friction, tidal damping) for the changes in tidal dynamics. I believe the article is a good example study for the influence of dam construction. There are some issues, however, needed to be well resolved before acceptance for publication.

Our reply: Thanks a lot for the positive assessment of our paper.

Major comments

1. The organization of the paper can be improved. For example, in section 4.1, the description of changed tidal amplitude and mean water level is followed by the analytical analysis of the tidal damping before detailing the model performance. I would suggest moving the later part in section 4.1 to section 4.2. Following a strategy as "observational analysis; model performance and validation; analysis of TGD's influence based on the model results".

Our reply: We do agree with the strategy you proposed. However, it is worth noting that the later part in section 4.1 actually described the observed tidal damping rate and residual water level slope based on the observed water levels in a monthly scale. Hence the whole section 4.1 only consists of observational analysis without including analytical analysis based on the analytical results. In the revised paper, we maintain the same structure of the paper.

2. The wording can be greatly improved. Some sentences have been mentioned again and again. For example, similar sentences as in L154-155 "we mainly concentrate on the tide-river dynamics under the impacts of TGD seasonal regulation over the entire reach of the Yangtze River estuary" can be found in multiple places, in the introduction, methods, results. Please revise them and make the text more concise. I would suggest mentioning such a sentence in the introduction and in the conclusion while avoiding repeating them in methods and results. Extensive minor grammar suggestions can be found in the minor comments.

Our reply: Many thanks for pointing this out. In the revised paper, we have removed the repeated sentences in the methods and results as suggested by the reviewer.

3. While I agreed that the discharge regulation affects the tidal dynamics, I am not

convinced that the influence of geometric or morphological change due to TGD is limited. The authors used 2007 bathymetric data, which might not reflect the alteration due to TGD considering the time-lag of 4-5 yrs in morphological response to the TGD. The morphological change can be more profound in recent years and it is well known that the reduced sediment delivery due to the trapping of TGD affects the erosion/deposition status of the Yangtze River delta. It is possible that the morphological change on the tidal might be less profound compared to the river discharge, but such a conclusion is not supported by the presented analysis. I would suggest rewording the related sentence regarding the influence of morphological change.

Our reply: We very much appreciate your comment with regard to potential impacts of the morphological adjustment (e.g., loss of floodplain storage by erosion) caused by the construction of the TGD on the tide-river dynamics. Indeed, the relative magnitude of morphological adjustment is likely to progressively increase due to the time-lag of morphological response and the rapid sedimentation in the reservoir (see Mei et al., 2018). Due to the lack of detailed bathymetry data before and after the TGD's operation, in this study we could not further analyze the impacts of morphological adjustment on the tide-river dynamics. In the revised paper, we have rewritten the sentence concerning the impacts of morphological change: "*The morphological change of Yangtze Estuary can be even more profound in recent years due to the continuous and accumulated impact from the TGD. Further adjustment of morphological change due to the sedimentation in the TGD could exert a considerable impact on the tide-river dynamics in the estuarine region (e.g., Du et al., 2018; Shaikh et al., 2018). Further study on the impact of morphological adjustment on the tide-river dynamics is required in the future.*" See lines 438-443 of the revised manuscript.

4. Regarding the TGD's influence on damping rate as shown in Fig. 3, could you explain why there so many jumping values (e.g., in Fig. 3a,c,d,e)? For an analytical solution with so many simplification assumptions, the response shall be in a much smoother way. Is such a jumping pattern observed in reality? I think it is important to clarify such abnormal features in your figures. Such types of not explained pattern also exist for figure 6-9, where there is a clear jumping pattern. Is it because you are using two manning coefficients for different regions?

Our reply: Figure 3 shows the observed tidal damping rate δ_H before and after the TGD closure for different reaches along the Yangtze estuary. These values are observations according to Equation (6) in the manuscript, rather than analytical results. The main reason that there exists a jumping pattern lies in the fact that the tidal damping rate δ_H are very small values (in terms of magnitude of -10^{-6} — 10^{-5}), thus small changes in observed tidal range would dramatically change the damping rate. In the revised paper, we have explicitly mentioned about this.

For the jumping behavior in Figures 6-9, this has to do with the adoption of two very different Manning-Strickler friction coefficient in the seaward and landward regions.

In the revised paper, to avoid such a sharp jump in the curves and to improve the model performance, we will adopt a friction coefficient of $K=80-55 \text{ m}^{1/3}\text{s}^{-1}$ (indicating a linear reduction of the friction coefficient) over the transitional reach ($x=32-52 \text{ km}$) in the analytical model. Figures R1-R4 below show the updated Figures 6-9 using a linear reduction of the friction coefficient in the transitional reach, where we observe a smooth transition of the analytically computed variables.

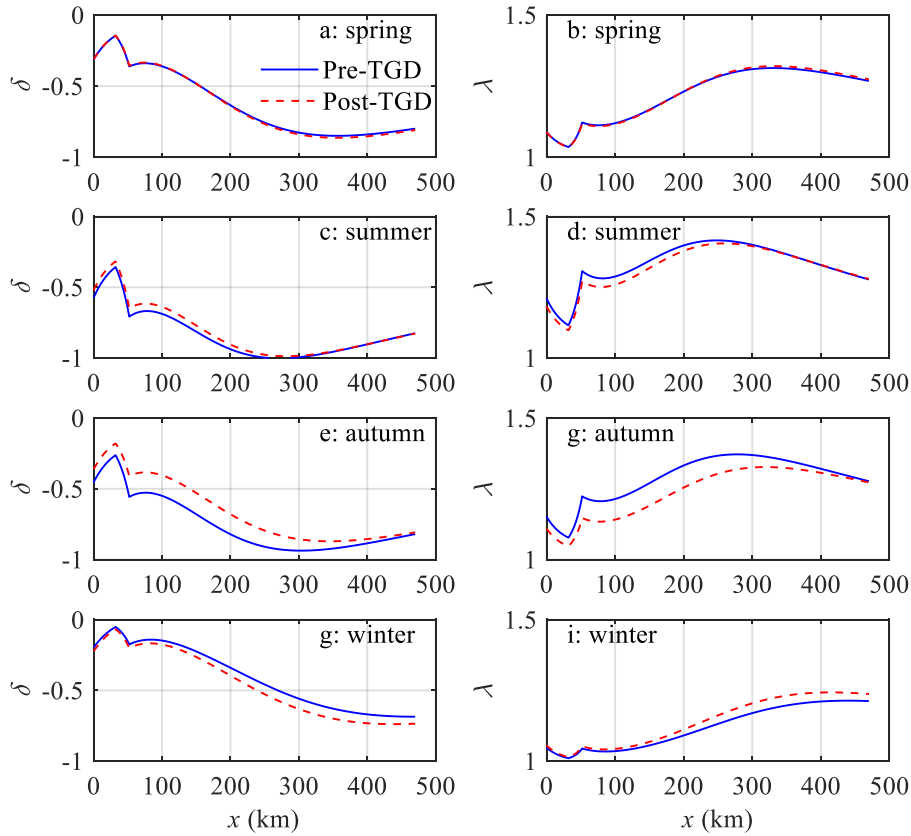


Figure R1. Longitudinal variability of simulated tidal damping number δ (a, c, e, g) and celerity number λ (b, d, g, i) along the Yangtze estuary in different seasons (spring: a, b; summer: c, d; autumn: e, g; winter: g, i) for both the pre-TGD and the post-TGD periods.

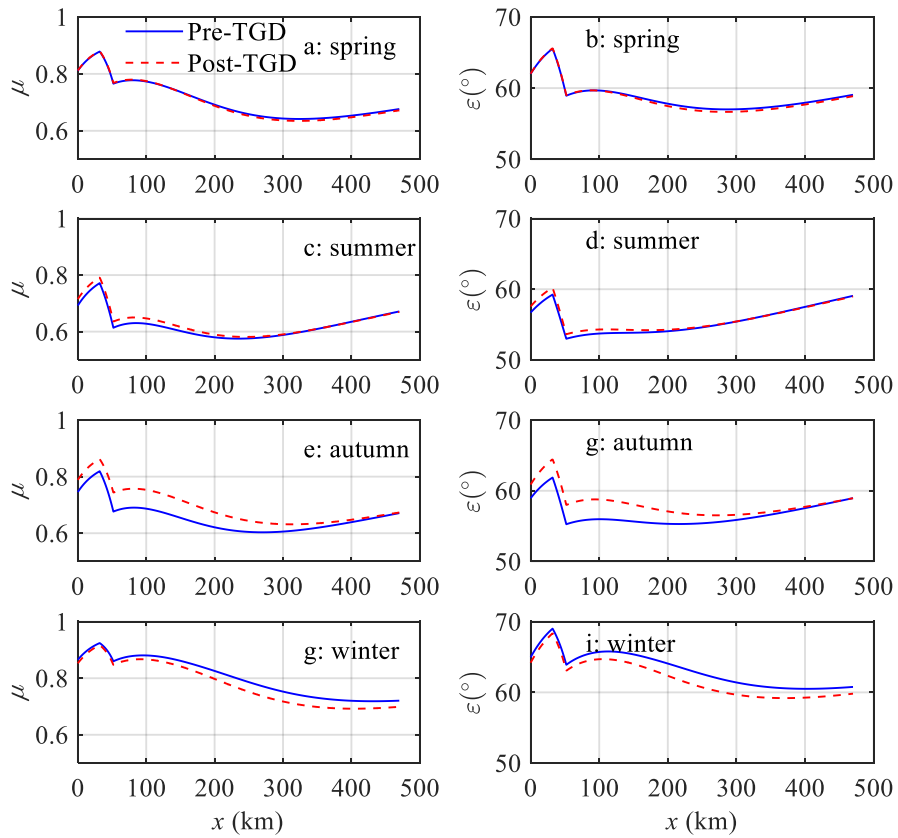


Figure R2. Longitudinal variability of simulated velocity number μ (a, c, e, g) and phase lag ε (b, d, g, i) along the Yangtze estuary in different seasons (spring: a, b; summer: c, d; autumn: e, g; winter: g, i) for both the pre-TGD and the post-TGD periods.

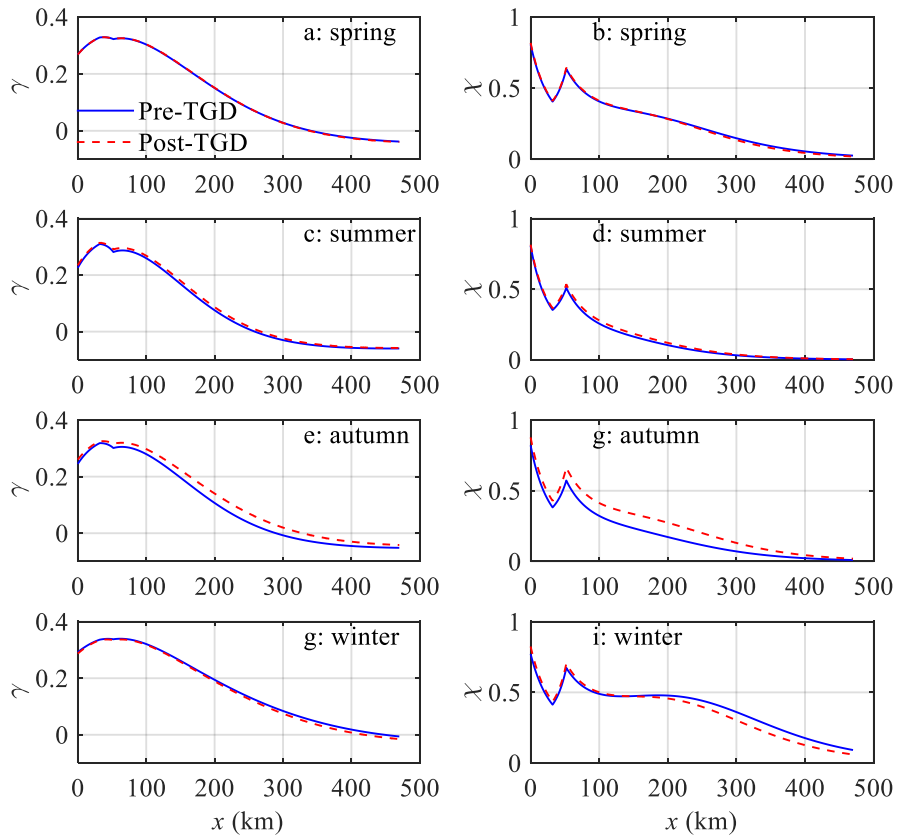


Figure R3. Longitudinal variability of simulated estuary shape number γ (a, c, e, g) and friction number χ (b, d, g, i) along the Yangtze estuary in different seasons (spring: a, b; summer: c, d; autumn: e, g; winter: g, i) for both the pre-TGD and the post-TGD periods.

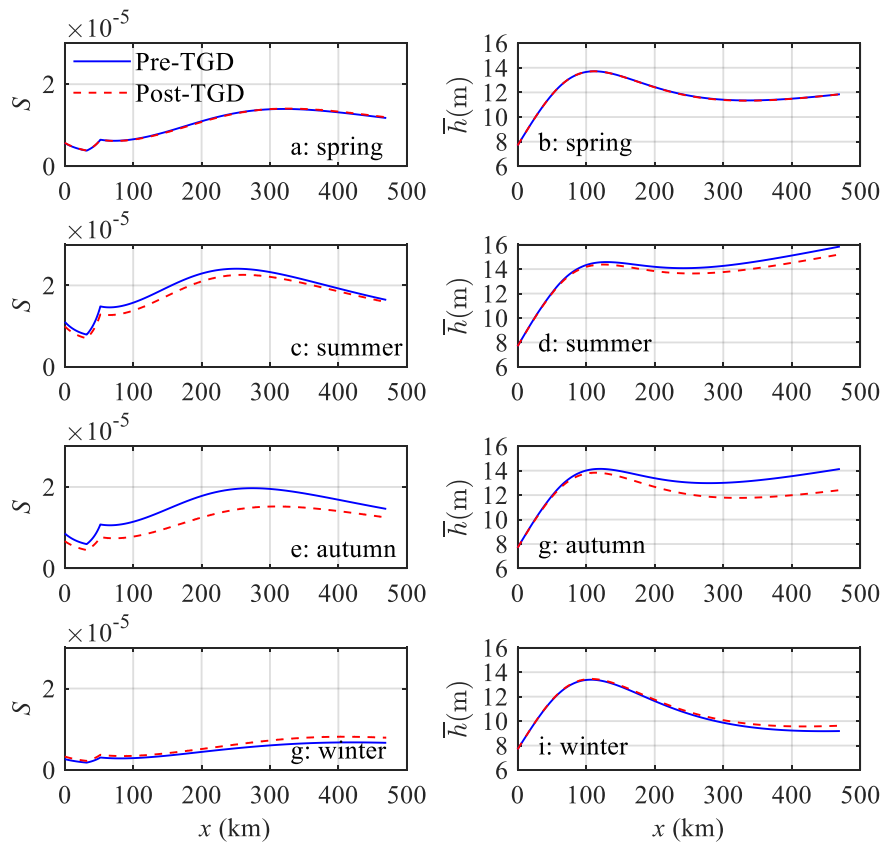


Figure R4. Longitudinal variability of simulated residual water level slope S (a, c, e, g) and water depth h (b, d, g, i) along the Yangtze estuary in different seasons (spring: a, b; summer: c, d; autumn: e, g; winter: g, i) for both the pre-TGD and the post-TGD periods.

5. As the major focus of this paper is to use the model to quantify the impact of freshwater discharge. It is vitally important to show the model can reproduce the change in tidal dynamics (e.g., tidal range) in response to varying freshwater discharge. For example, a plot showing the observed change of tidal range (using the amplitude of M2 would be better) as a function of freshwater input at selected stations, together with another line showing the modeled amplitude as a function of river discharge.

Our reply: As we mentioned in the introduction part, the main purpose of this paper lies in quantifying the impacts of TGD's seasonal regulation on the tide-river dynamics over the entire reach of the Yangtze River estuary. Concerning the impacts of varying freshwater discharge on the tide-river dynamics, the reviewer can kindly refer to our recent publication in the journal of Hydrology and Earth System Sciences (in discussion): Cai, H., Savenije, H. H. G., Garel, E., Zhang, X., Guo, L., Zhang, M., Liu, F., and Yang, Q., 2018. Seasonal behaviour of tidal damping and residual water level slope in the Yangtze River estuary: identifying the critical position and river discharge for maximum tidal damping, *Hydrol. Earth Syst. Sci. Discuss.*,

<https://doi.org/10.5194/hess-2018-524>, in review.

6. For the captions of many figures, it is necessary to detail what each data point represent for. For example, in Figure 5, it not clear to me how each data point is obtained, is it monthly mean value?

Our reply: These are monthly averaged values. In the revised paper, we have clarified the plotted data in the captions of all the figures. For instance, we shall modify the caption of the Figure 5 as “*Comparison of monthly averaged values for (a, b) analytically computed tidal amplitude η and (c, d) residual water level \bar{Z} against the observations in the Yangtze River estuary for the pre-TGD period (1979–1984) and post-TGD period (2003–2014).*” See lines 356-359 of the revised manuscript.

Minor comments

L44: “to the extent” here reads awkward. Please consider to revise it.

Our reply: We have replaced “to the extent that” with “so that” in the revised paper. See line 44 of the revised manuscript.

L54: a recent work by Du et al. (2018) might be a good reference in concern of the geomorphic constraints on tidal dynamics.

Our reply: Thank you for pointing this out. In the revised paper, we have included this recent work. See line 55 and line 441 of the revised manuscript.

L55: suggest to change “including spring-neap tidal fluctuations as well as seasonal varying discharge” to “in timescale ranging from a fortnight to season”

Our reply: We agree with your suggestion. See line 57 of the revised manuscript.

L57: change “of the river” to “of a river”

Our reply: We agree with your comment. See line 58 of the revised manuscript.

L58: delete “being”, only those that have already been built can cause changes in downstream freshwater discharge.

Our reply: We agree with your comment.

L64: suggest moving the part “such as xxxx” forward to as “human intervention, such as xxxx, which are xxxx”

Our reply: We agree with your comment. See lines 63-66 of the revised manuscript.

L68: suggest changing “a large river” to “the largest river in China in terms of mean discharge” to emphasize the importance of Yangtze River.

Our reply: We agree with your comment. See line 70 of the revised manuscript.

L92: suggest changing “that have been mainly been concerned with” to “on”, making it more concise.

Our reply: We agree with your comment.

L114: change “the TGD seasonal regulation effect” to “the effect of TGD seasonal regulation”

Our reply: We agree with your comment. See line 115 of the revised manuscript.

L119, L121: suggest using past tense of phase, to be consistent to the phase you used at the beginning, where you used “adopted”.

Our reply: We agree with your comment.

L138: change “Downstream of” to “Downstream”

Our reply: We agree with your comment. See line 140 of the revised manuscript.

L143: change “discharge” to “was discharged”

Our reply: We agree with your comment. See line 146 of the revised manuscript.

L148: change “a tidal range that extends up to 4.6m” to “a tidal range of up to 4.6 m”

Our reply: We agree with your comment. See line 150 of the revised manuscript.

L157: Delete “Sketch”, it is actually a map, not a sketch one. Suggest changing “displaying the location of gauging and hydrological stations” to “with the location of tidal gauging and hydrological stations shown with black solid circles and rec solid rectangles”.

Our reply: We agree with your comment. See lines 155-157 of the revised manuscript.

L168: change “difference of” to “difference between”

Our reply: We agree with your comment. See line 167 of the revised manuscript.

L169: “and a half” to “and dividing by two”.

Our reply: We agree with your comment. See line 168 of the revised manuscript.

L170: “water levels of xx stations” to “water level at xx stations”

Our reply: We agree with your comment. See line 169 of the revised manuscript.

L206: will the solution for rectangle lateral shape channel be different with those with a V-shape? It is better to state here why such an assumption is valid as most part of estuary is not rectangle shape but v-shape.

Our reply: We agree that most small estuaries are characterized with a V-shaped cross section. However, the Yangtze estuary is extremely large with the mouth width of around 90 km, and the width of river channel is convergence from around 10 km in the downstream to around 2-3 km in the upstream. In contrast, the depth is only at around 10-20 m. In this sense we believe the rectangular shape assumption is reasonable. Following the suggestion of reviewer, we have revised the sentence as “*We further assume a nearly rectangular cross-section, considering a large width to*”

depth ratio; hence, the tidally averaged depth is given by $\bar{h} = \bar{A}/\bar{B}$ and the cross-sectional area variability can be primarily attributed to the change in depth.” See lines 204-207 of the revised manuscript.

L214-217: These symbols are not used for the four number and it is not appropriate to use "where" here. I suggest to move it as a note under the table 1, or express the formula for each number explicitly in the text (say, each number is described with its corresponding formula in the text).

Our reply: In the revised paper, we have revised the sentence as: “*The definitions of these four variables are defined in Table 1, where η is the tidal amplitude, v is the velocity amplitude, U_r is the river flow velocity, ω is the tidal frequency, r_s is the storage width ratio accounting for the effect of storage area (i.e. tidal flats or salt marshes), and c_0 is the classical wave celerity defined as $c_0 = \sqrt{g\bar{h}/r_s}$.*” See lines 215-219 of the revised manuscript.

L280: “in upstream stations” to “at upstream stations”

Our reply: We agree with your comment. See line 284 of the revised manuscript.

L302-309: Isn't it necessary to describe why some segments has seen little change or even decrease? It is confusing. Why increased damping denotes weaker friction? For classic understanding, it is thought larger friction lead to a higher damping rate.

Our reply: Here it should be noted that the value of damping rate δ_H is negative, thus a higher damping rate indicates less friction rather than larger friction.

Figure 5: what does each data point stand for? Monthly value? Or yearly value?

Our reply: They are monthly averaged values. In the revised paper, we have explicitly mentioned this in the caption of the figure. See lines 356-359 of the revised manuscript.

Section 4.3: the second part in section 4.1 is suggested to move into section 4.3.

Our reply: We do not agree this comment since the second part in section 4.1 describing the observed tidal damping rate and residual water level slope as a function of observed freshwater discharge at Datong hydrological station. This part still belongs to the observational analysis rather than the analytical analysis.

L373: “identify” seems not a good word here.

Our reply: In the revised paper, we have replaced “identify” with “observe”. See line 385 of the revised manuscript.

L383: in “the larger the freshwater discharge is, the smaller the velocity number and the phase lag are.”, suggest changing as “the larger the freshwater discharge, the smaller the velocity number and the phase lag.”

Our reply: We agree with your comment. See lines 394-395 of the revised

manuscript.

Figure 6: why there is sharply jumping in the curve, due to different manning coefficient?

Our reply: Indeed, the discontinuous jump has to do with the adoption of two very different Manning-Strickler friction coefficient. To avoid such a sharp jump in the curve, in the revised paper, we adopt a friction coefficient of $K=80-55 \text{ m}^{1/3}\text{s}^{-1}$ (indicating a linear reduction of the friction coefficient) over the transitional reach ($x=32-52 \text{ km}$).

L416: “the river immediately downstream eroded” to “the river bed immediately downstream was eroded”

Our reply: We agree with your comment. See lines 426-427 of the revised manuscript.

L426: “therefore” may be a better word than “consequently”

Our reply: This sentence has been deleted in the revised manuscript.

L463-466: this whole sentence reads awkward. Suggesting changing “where the tidal influence dominates that of the freshwater discharge” to “where tidal influence overwhelms the influence from freshwater discharge”.

Our reply: We agree with your comment. See line 477-448 of the revised manuscript.

L500: “drawn lines” to “solid lines”

Our reply: We agree with your comment. See line 516 of the revised manuscript.

L519: it is not clear how you determine the value “20-yr” and “10-yr” here.

Our reply: Generally, these values should be determined based on the long-term time series of the monthly averaged high-water levels. To avoid confusing, we have revised the sentence as: “*The corresponding flood prevention standard, therefore, is reduced due to the increased high-water level (see also Nakayama and Shankman, 2013).*” See lines 535-536 of the revised manuscript.

L574: suggest changing “as a significant case study” to “as an example”

Our reply: We agree with your comment. See line 600 of the revised manuscript.

Responses to comments by Reviewer #2

We thank Dr. Lewis's comments of our work. In this rebuttal, we have addressed all the comments formulated by the Reviewer by replying (in black) to his remarks (in blue). The lines numbers in this rebuttal refer to the revised version of the manuscript.

General comments:

A very interesting study, with applications to all "downstream consequences from land management practice (e.g. reservoirs, hydro-electric, flood risk mitigation). I think the article is great and worthy of publication, but I have some concerns – listed below. Applying an analytical model to find the downstream change to volume of a river due to upstream water collection (the three gorges dam) is neat – but I am unsure how this can be used to assess impact to biology.

Our reply: Thanks a lot for the reviewer's positive evaluation of our manuscript. Due to the fact that in this study we mainly focus on the impacts of freshwater regulation of TGD on spatial-temporal patterns of tide-river dynamics in the Yangtze River estuary, we did not provide details concerning the TGD's impact on biology in the paper. However, we do mention the possible influence of TGD's operation on ecology in the sections of ABSTRACT and INTRODUCTION. In particular, the results obtained from this study can further be used to assess the impacts of TGD's operation on salt intrusion (as a general predictor of the aquatic ecosystem health in estuarine environment) when combined with an ecological or salt intrusion model. This is further elaborated in the DISCUSSION part (see Section 5.4 in the manuscript). In the revised paper, we have explicitly mentioned that "*However, to quantify the potential impacts of TGD's operation on salt intrusion and related aquatic ecosystem health in general, it is required to couple the hydrodynamic model to the ecological or salt intrusion model (e.g., Qiu and Zhu, 2103; Cai et al., 2015).*" See lines 583-586 of the revised manuscript.

Major comments

1. Inter-annual variability. I think some effort to resolve inter-annual variability would have been nice. Standard deviation could be added to the mean values in Figure 11 - and then a conclusion of "significant change between months 7 to 11" can be made with confidence. At present such a statement cannot be made: Significant compared to what? Where is the test of significance? At best the authors can say "the change in the mean is clear for months 7-10". If Table 2 had more data added, i.e. how the monthly mean changes each year – it would be nice. Certainly the data is sufficient (it spans multiple years), and so the inter-annual variability can be added to Figure 11. That said, perhaps the authors can defend my comment here?

Our reply: We thank the reviewer for this comment. Indeed, it is better to resolve the inter-annual variability. In the revised paper, we have included the standard deviation information in Figure 11 (see Figure R1 below).

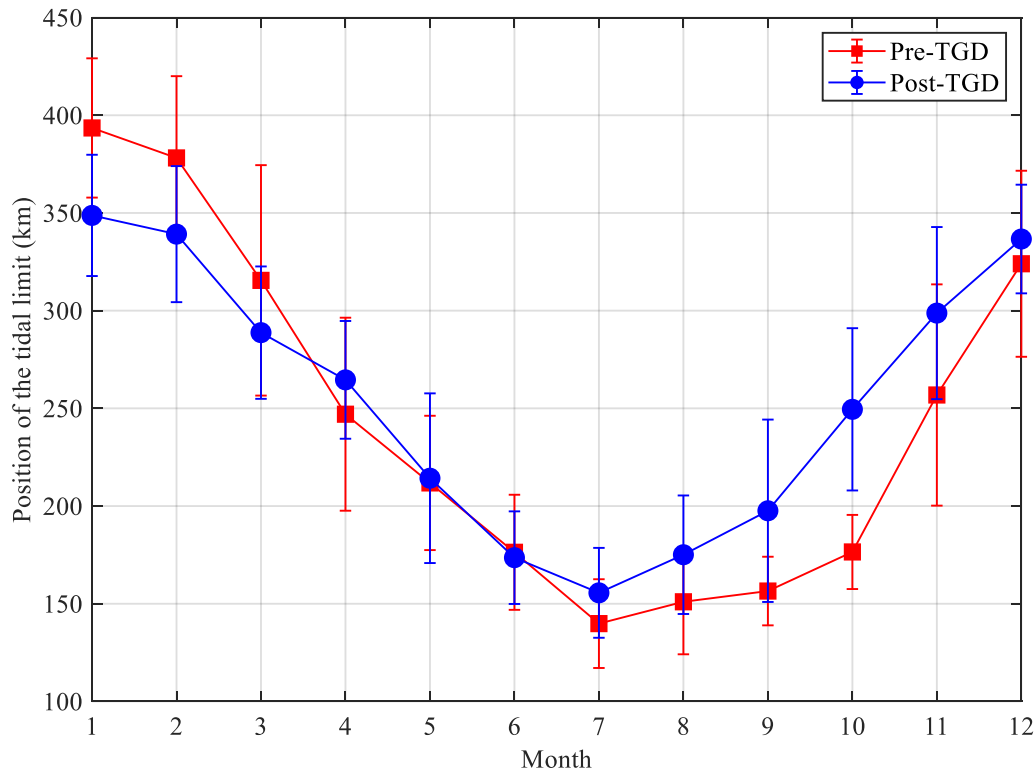


Figure R1. Temporal variation of the position of the tidal limit relative to the TSG station for both the pre-TGD and the post-TGD periods. The vertical error bar at each data point indicates the standard deviation of the analytically computed time series.

2. Sub-monthly variability impact. Another concern I have is the resolution of the model. Is the frequency of boundary forcing information sufficient to resolve extreme events? For example, daily-averaged flow rates were found to be insufficient to resolve flood risk and water quality within estuary hydrodynamic models (e.g. Robins, P.E., Lewis, M.J., Freer, J., Cooper, D.M., Skinner, C.J. and Coulthard, T.J., 2018. Improving estuary models by reducing uncertainties associated with river flows. *Estuarine, Coastal and Shelf Science*, 207, pp.63-73.) I guess I am simply asking: you have monthly means, but how does this down-scale to hourly means, which are likely to be important for impact to wildlife and estuary impact? For this second comment, perhaps a sensitivity test is needed to prove to the reader that you can take coarse river data and resolve estuary impact. However, perhaps this can also be defended by the authors?

Our reply: Due to the fact that the main purpose of this study lies in quantifying the impacts of TGD's seasonal regulation on the tide-river dynamics over the entire reach of the Yangtze River estuary, thus we adopted the monthly averaged river discharge conditions. This is possible to down-scale to the tidally averaged means since the proposed analytical model is obtained based on the tidally averaged conditions. For such a kind of application using tidally averaged means, the reviewer can kindly refer to our previous publications of Cai et al. (2014, 2016). However, the model cannot be used to understand the impacts of hourly varying freshwater discharge on the tide-river dynamics because of model limitation. To resolve extreme events and their

impacts on flood control and water quality, as suggested by the reviewer (e.g., Robins et al., 2018), it is required to use a high-resolution numerical model adopting high-resolution boundary conditions (e.g., hourly mean river discharge).

3. Assumptions of river geometry variability. For the analytical solution method – how is river width treated for application to volume temporally variance? Is an assumption made about the river being canalised? i.e. constant bank full width? Or is there an associated flood plan? How is river depth calculated? If so, how does this effect your results?

Our reply: Indeed, in the analytical model we simplified the channel geometry to be in the shape of rectangular geometry. This means that the channel width is assumed to be time-invariant, while the water depth is variable as a function of tidal and riverine forcing. Such an assumption is particularly reasonable since the Yangtze River estuary is extremely large with the mouth width of around 90 km, and the width of river channel is convergent from around 10 km in the downstream section to around 2-3 km in the upstream section. On the other hand, the depth is only at around 10-20 m along the main course of the estuary. Consequently, the width to depth ratio is large so that the cross-sectional area variability can be primarily caused by the depth variability. The possible influence of storage area (i.e. flood plain and tidal flats) is taken into consideration by introducing the parameter of the storage width ratio r_s (i.e., the ratio of the storage width to the averaged stream width). Such a kind of rectangular shape assumption has been used in many previous studies (e.g., Van Rijn, 2011, Toffolon and Savenije, 2011, Cai et al., 2014, 2016). In the revised paper, we have clarified such an assumption: “*We further assume a nearly rectangular cross-section, considering a large width to depth ratio; hence, the tidally averaged depth is given by $\bar{h} = \bar{A}/\bar{B}$ and the cross-sectional area variability can be primarily attributed to the change in depth.*” See lines 204-207 of the revised manuscript.

References:

- Cai, H., Savenije, H. H. G., and Toffolon, M.: Linking the river to the estuary, influence of river discharge on tidal damping, *Hydrol. Earth Syst. Sci.*, 18(1), 287-304, <https://doi.org/10.5194/hess-18-287-2014>, 2014.
- Cai, H., Savenije, H.H.G., Zuo, S., Jiang, C., and Chua, V.: A predictive model for salt intrusion in estuaries applied to the Yangtze estuary, *J. Hydrol.*, 529, 1336-1349, <https://doi.org/10.1016/j.jhydrol.2015.08.050>, 2015.
- Cai, H., Savenije, H. H. G., Jiang, C. Zhao L., Yang Q.: Analytical approach for determining the mean water level profile in an estuary with substantial fresh water discharge, *Hydrol. Earth Syst. Sci.*, 20, 1-19, <https://doi.org/10.5194/hess-20-1-2016>, 2016.
- Cai, H., Savenije, H. H. G., Garel, E., Zhang, X., Guo, L., Zhang, M., Liu, F., and Yang, Q., 2018. Seasonal behaviour of tidal damping and residual water level slope in the Yangtze River estuary: identifying the critical position and river discharge for maximum tidal damping, *Hydrol. Earth Syst. Sci. Discuss.*, <https://doi.org/10.5194/hess-2018-524>, in review.

- Mei, X., Dai, Z., Darby, S. E., Gao, S., Wang, J., Jiang, W.: Modulation of extreme flood levels by impoundment significantly offset by floodplain loss downstream of the Three Gorges Dam. *Geophys. Res. Lett.*, 45, 3147–3155, <https://doi.org/10.1002/2017GL076935>, 2018.
- Nakayama, T., Shankman, D.: Impact of the Three-Gorges Dam and water transfer project on Changjiang floods. *Global Planet Change*, 100, 38-50, <https://doi.org/10.1016/j.gloplacha.2012.10.004>, 2013.
- Shaikh, B.Y., Bansal, R.K., Das, S.K.: Propagation of tidal wave in coastal terrains with complex bed geometry. *Environmental Processes*, 5(3), 519-537, 2018.
- Qiu, C. and Zhu., J.: Influence of seasonal runoff regulation by the Three Gorges Reservoir on saltwater intrusion in the Changjiang River Estuary, *Cont. Shelf Res.*, 71, 16-26, <https://doi.org/10.1016/j.csr.2013.09.024>, 2013.
- Robins, P.E., Lewis, M.J., Freer, J., Cooper, D.M., Skinner, C.J., Coulthard, T.J.: Improving estuary models by reducing uncertainties associated with river flows, *Estuar. Coast. Shelf S.*, 207, 63-73, <https://doi.org/10.1016/j.ecss.2018.02.015>, 2018.
- Toffolon, M., Savenije, H. H. G.: Revisiting linearized one-dimensional tidal propagation, *J. Geophys. Res.* 116, C07007, <https://doi.org/10.1029/2010JC006616>, 2011.
- van Rijn, L. C.: Analytical and numerical analysis of tides and salinities in estuaries; part I: Tidal wave propagation in convergent estuaries, *Ocean Dynam.* 61(11), 1719–1741, <https://doi.org/10.1007/s10236-011-0453-0>, 2011.

1 **Impacts of Three Gorges Dam’s operation on spatial-temporal**
2 **patterns of tide-river dynamics in the Yangtze River estuary, China**

3 Huayang Cai^{1,2}, Xianyi Zhang¹, Leicheng Guo², Min Zhang^{3,*}, Feng Liu¹, Qingshu
4 Yang¹

5
6 *1. Institute of Estuarine and Coastal Research, School of Marine Engineering and*
7 *Technology, Sun Yat-sen University, Guangzhou, China*

8 *2. State Key Laboratory of Estuarine and Coastal Research, East China Normal*
9 *University, Shanghai, China*

10 *3. Shanghai Normal University, School of Environmental and Geographical Sciences,*
11 *Shanghai, China*

12 **Corresponding author:** Min Zhang

13 **Corresponding author’s E-mail:** zhangmin@shnu.edu.cn
14

15 **Key points**

16 1. Impacts of TGD operation on tide-river dynamics are quantified using an
17 analytical model.

18 2. The strongest impacts occurred during autumn and winter due to the seasonal
19 freshwater regulation by TGD.

20 3. The alteration of tide-river dynamics may exert considerable impacts on
21 sustainable water resource management in dam-controlled estuaries.

22

23

24

25

26

27

28 **Abstract**

29 The Three Gorges Dam (TGD), located in the mainstream of the Yangtze River, is the
30 world's largest hydroelectric station in terms of installed power capacity. It was
31 demonstrated that the TGD had caused considerable modifications in the downstream
32 freshwater discharge due to its seasonal operation mode of multiple utilisation for
33 flood control, irrigation, and power generation. To understand the impacts of the
34 freshwater regulation of TGD, an analytical model is adopted to explore how the
35 operation of TGD may affect the spatial-temporal patterns of tide-river dynamics in
36 the Yangtze River estuary. We evaluated the effect of TGD by comparing the changes
37 in major tide-river dynamics in the post-TGD period (2003–2014) with those in the
38 pre-TGD period (1979–1984). The results indicate that the strongest impacts occurred
39 during the autumn and winter, corresponding to a substantial reduction in freshwater
40 discharge during the wet-to-dry transition period and slightly increased discharge
41 during the dry season. The underlying mechanism leading to changes in the tide-river
42 dynamics lies in the alteration of freshwater discharge, while the impact of geometric
43 change is minimal. Overall, the results suggest that the spatial-temporal patterns of
44 tide-river dynamics is sensible to the freshwater regulation of the TGD, ~~too~~ ~~the~~
45 ~~extent~~ that the ecosystem function of the estuary may undergo profound disturbances.
46 The results obtained from this study can be used to set scientific guidelines for water
47 resource management (e.g. navigation, flood control, salt intrusion) in dam-controlled
48 estuarine systems.

49 **Key words:** seasonal freshwater regulation, Three Gorges Dam, analytical model,

50 tide-river dynamics, Yangtze River estuary

51 1. Introduction

52 Estuaries are transition zones where river meets ocean (Savenije, 2012). Tide-river
53 interactions, a result of both hydrologic drivers and geomorphic constraints, are
54 highly dynamic in estuaries (Buschman et al., 2009; Sassi and Hoitink, 2013; Guo et
55 al., 2015; Cai et al., 2016; Hoitink and Jay, 2016; Hoitink et al., 2017; [Du et al., 2018](#)).

56 In natural conditions, they usually experience a wide range of temporal variations, [in](#)
57 [timescale ranging from a fortnight to season including spring neap tidal fluctuations as](#)
58 [well as seasonal varying discharges](#) (e.g. Zhang et al., 2018). Human intervention,
59 such as dam construction in the upstream parts of [the a](#) river and the growing number
60 of water conservancy projects [being](#) built along large rivers (such as freshwater
61 withdrawal), have caused seasonal changes in downstream freshwater discharge
62 delivery, leading to adjustments in the function of fluvial and estuarine hydrology (e.g.
63 Lu et al., 2011; Mei et al., 2015; Dai et al., 2017). Consequently, it is important to
64 understand the impacts of large-scale human intervention, [such as flood control,](#)
65 [navigation, salt intrusion, and freshwater withdrawal](#), which are relevant not only to
66 tide-river dynamics and riparian ecology but also to sustainable water resource
67 management in general, [such as flood control, navigation, salt intrusion, and](#)
68 [freshwater withdrawal](#).

69

70 River discharge generally fluctuates following a wet-dry cycle due to the seasonal
71 variation of precipitation in the upstream river basin. For instance, the Yangtze River,

带格式的: 缩进: 首行缩进: 0 字符

设置了格式: 字体: (默认) Times New Roman, 小四, 字体
颜色: 文字 1, 英语(英国)

72 [the largest river in China in terms of mean discharge](#) ~~large river~~, which flows into the
73 East China Sea, has a maximum river discharge during summer in July and a low
74 value during winter in January, with a maximum discharge difference of
75 approximately 38,000 m³/s (Cai et al., 2016). Similar seasonal variations are also
76 identified in other large rivers in eastern and southern Asia, such as the Mekong River
77 in Vietnam, Ganges River in India, and Pearl River in China, under the influence of a
78 monsoon climate. However, most large rivers have been significantly dammed at the
79 central and upper reaches in recent decades, dramatically modifying stream hydrology
80 and sediment delivery, resulting in changes in hydraulics and river delta development
81 trend at the lower reaches (e.g. Räsänen et al, 2017; Rahman et al., 2018; Liu et al.,
82 2018). Due to the fact that the response of tide-river interactions to the impacts of
83 dams are diverse and non-uniform and that many more dams are to be built in the
84 future, the impacts of the hydrodynamic interactions between tidal waves and
85 seasonal river flows from natural variations and anthropogenic activities have become
86 a common focus in international hydraulic research, especially in large tidal rivers.

87

88 The Yangtze River estuary, located near the coastal area of East China Sea, is one of
89 the largest estuaries in Asia. In the mouth of the Yangtze River estuary, bifurcation
90 occurs and the characteristics of tides have been broadly investigated in previous
91 studies (e.g. Zhang et al., 2012; Lu et al., 2015; Alebregtse and Swart, 2016).
92 However, in these studies, river influences are usually neglected. In recent years, the
93 processes of nonlinear interactions between tidal wave and river flow in the Yangtze

94 River estuary have received increasing attention (e.g. Guo et al., 2015; Zhang et al.,
95 2015a, b; Cai et al., 2016; Kuang et al., 2017; Zhang et al., 2018). However, recent
96 studies ~~that have been mainly concerned with~~ on tidal properties, such as asymmetry,
97 changes near the mouth area, and seasonal variations in tidal wave propagation and
98 fluvial effects over the entire 600 km of the tidal river, up to the tidal limit of the
99 Datong hydrological station, have been limited. In addition, the operation of the Three
100 Gorges Dam (TGD), the largest dam in the world, has substantially affected the
101 downstream river hydrology and sediment delivery. There is a variety of debate
102 regarding the potential impacts of TGD on the downstream river morphology,
103 hydrology, and ecology, since the underlying mechanism of the impact of the TGD is
104 not fully understood. Specifically, the TGD operation has altered the downstream
105 fluvial discharge and water levels on the seasonal scale, directly following the
106 reservoir seasonal impounding and release of water volume (e.g. Chen et al., 2016;
107 Guo et al., 2018). However, the impacts of seasonal freshwater regulation by the TGD
108 on the spatial-temporal tide-river dynamics in the downstream estuarine area have not
109 been systematically investigated. For example, during the dry season TGD operation
110 increased the multi-year monthly averaged river discharge at Datong station from
111 $9520 \text{ m}^3 \cdot \text{s}^{-1}$ to $12896 \text{ m}^3 \cdot \text{s}^{-1}$ in January, while during wet season the regulation
112 reduced the river discharge from $49900 \text{ m}^3 \cdot \text{s}^{-1}$ to $44367 \text{ m}^3 \cdot \text{s}^{-1}$ in July during the pre-
113 and post- TGD period.

114

115 In this study, for the first time, the spatial-temporal variations in the hydrodynamic

116 processes due to the interactions of tidal flow and fluvial discharge in the Yangtze
117 River estuary caused by natural forcing and human intervention were studied, with
118 specific focus on ~~the effect of TGD seasonal regulation~~the TGD seasonal regulation
119 ~~effect~~. Here, we adopted a well-developed analytical model proposed by Cai et al.
120 (2014a, 2016) to investigate the spatial-temporal patterns of tide-river dynamics in the
121 entire Yangtze River estuary and quantify the impacts of the TGD operation. In the
122 following sections, we introduce the study site of the Yangtze River estuary. This is
123 followed by a description of the available data and analytical model of tide-river
124 dynamics in Section 3. Subsequently, we ~~apply~~applied the model to the Yangtze
125 River estuary, where the TGD has operated since 2003 (Section 4). In particular, we
126 ~~explored~~ the alteration of the tide-river dynamics after the TGD closure and
127 summarise the impacts of the TGD on the spatial-temporal patterns of tide-river
128 dynamics. The impacts of channel geometry and river discharge alterations on
129 tide-river dynamics as well as the implications for sustainable water resource
130 management ~~are~~were then discussed in Section 5. Finally, some key findings ~~are~~
131 were addressed in Section 6.

132

133 **2. Overview of the Yangtze River estuary**

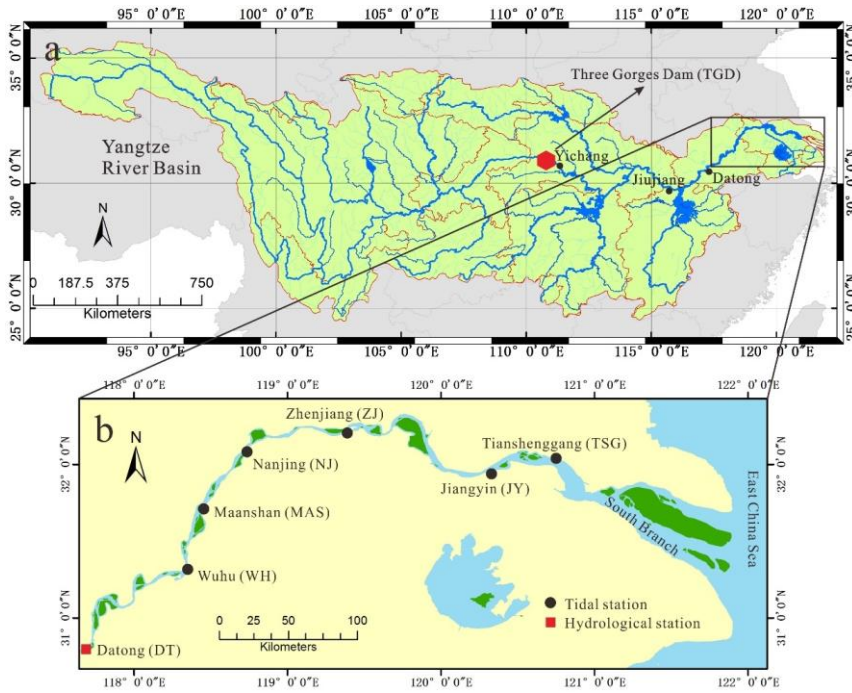
134 The Yangtze River, flowing from west to east in central China, is one of the world's
135 most important rivers due to its great economic and social relevance. It has a length of
136 about 6300 km and a basin area of about 190,000 km² (Figure 1a). The Yangtze River
137 basin is geographically divided into three parts, the upper, central, and lower

138 sub-basins, and contains an estuary area with partitions at Yichang, Jiujiang, and
139 Datong (DT), respectively (Figure 1a). Of concern in this study are the impacts of the
140 Three Gorges Dam (TGD), the world's largest dam, on the spatial-temporal patterns of
141 tide-river dynamics in the estuarine area. It is located about 45 km upstream of
142 Yichang (Figure 1a). The TGD project began in 2003; by 2009, when full operations
143 began, the total water storage capacity rose up to $\sim 40 \text{ km}^3$, equivalent to 5% of the
144 Yangtze's annual discharge. Downstream of the DT station, where the tidal limit is
145 located, the Yangtze River estuary extends $\sim 630 \text{ km}$ to the seaward end of the South
146 Branch. Wuhu (WH), Maanshan (MAS), Nanjing (NJ), Zhenjiang (ZJ), Jiangyin (JY),
147 and Tianshenggang (TSG) are the major gauging stations along the mainstream in the
148 seaward direction (Figure 1b). Under the control of the Asian monsoon climate, river
149 discharges show distinct seasonal patterns. In 1979–2012, more than 70% of
150 freshwater was discharged at DT occurred during summer (May–October).

151

152 Apart from river flows, tidal waves are also recognised as the major sources of energy
153 for hydrodynamics in the Yangtze River estuary, which is characterised by a meso-tide
154 with a tidal range that extends of up to $\sim 4.6 \text{ m}$ and a mean tidal range of $\sim 2.7 \text{ m}$ near
155 the estuary mouth. According to the observation in the Gaoqiaoju tidal gauging station
156 (1950–2012), the averaged ebb tide duration (7.5 h) is a bit longer than the averaged
157 flood tide duration (5 h), indicating an irregular semidiurnal character (Zhang et al.,
158 2012). Unlike previous studies focusing on tidal hydrodynamics near the estuary
159 mouth, or water and sediment alterations since the beginning of TGD operation, here,

160 we mainly concentrate on the tide-river dynamics under the impacts of TGD seasonal
161 regulation over the entire reach of the Yangtze River estuary.



162
163 Figure 1. ~~Sketch M~~maps of the Yangtze River basin (a) and Yangtze River estuary (b),
164 ~~with the location of tidal gauging and hydrological stations shown with black solid~~
165 ~~circles and reed solid rectangles~~ displaying the location of gauging and hydrological
166 ~~stations.~~

167

168 3. Data and Methodology

169 3.1 Source of Data

170 To quantitatively investigate the relationship between freshwater discharge regulation
171 caused by the TGD operation and the tide-river dynamics, monthly averaged

172 hydrological data for both pre-TGD (1979–1984) and post-TGD (2003–2014) periods
173 of tidal range and water level from the above-mentioned six tidal gauging stations
174 along the Yangtze River estuary were collected. They were published by the Yangtze
175 Hydrology Bureau of the People's Republic of China. The monthly averaged tidal
176 amplitude is determined by averaging the daily difference ~~of-between~~ high and low
177 water levels and ~~dividing by two-half~~. To correctly quantify the residual water level
178 along the Yangtze estuary, locally measured water levels ~~of-at~~ different gauging
179 stations are corrected to the national mean sea level of Huanghai 1985.

180

181 **3.2 Analytical model for tide-river dynamics**

182 **3.2.1 Basic equations**

183 In tidal rivers, the tidally averaged water level (i.e. residual water level) depicts a
184 steady gradient, which usually increases with freshwater discharge (e.g. Sassi and
185 Hoitink, 2013). The key to deriving the dynamics of the residual water level lies in the
186 one-dimensional momentum equation, which can be expressed as (e.g. Savenije, 2005,
187 2012):

$$188 \quad \frac{\partial U}{\partial t} + U \frac{\partial U}{\partial x} + g \frac{\partial Z}{\partial x} + \frac{gh}{2\rho} \frac{\partial \rho}{\partial x} + g \frac{U|U|}{K^2 h^{4/3}} = 0, \quad (1)$$

189 where U is the cross-sectional averaged velocity, Z is the free surface elevation, h is
190 the water depth, g is the acceleration due to gravity, t is the time, ρ is the water density,
191 x is the longitudinal coordinate directed landward, and K is the Manning-Strickler
192 friction coefficient. It was demonstrated that in the subtidal momentum balance, the
193 residual water level slope is primarily balanced by the residual friction term (Vignoli

194 et al., 2003; Buschman et al., 2009; Cai et al., 2014a, for a detailed derivation, readers
 195 can refer to the Appendix A):

$$196 \quad \frac{\overline{\partial Z}}{\partial x} = -\frac{\overline{U|U|}}{K^2 h^{4/3}} \quad (22)$$

197
 198 where the overbars indicate the tidal average. For a single channel with the residual
 199 water level set to 0 at the estuary mouth (i.e. $\bar{Z} = 0$ at $x = 0$), the integration of

200 Equation (22) leads to an analytical expression for the residual water level

$$201 \quad \bar{Z}(x) = -\int_0^x \frac{\overline{\partial Z}}{\partial x} = -\int_0^x \frac{\overline{U|U|}}{K^2 h^{4/3}} \quad (33)$$

202 To derive the analytical solutions for tide-river dynamics, we assume that the
 203 longitudinal variation of cross-sectional area \bar{A} and width \bar{B} can be described by the
 204 following exponential functions (see also Toffolon et al., 2006; Cai et al., 2014a):

$$205 \quad \bar{A} = \bar{A}_r + (\bar{A}_0 - \bar{A}_r) \exp\left(-\frac{x}{a}\right), \quad (44)$$

$$206 \quad \bar{B} = \bar{B}_r + (\bar{B}_0 - \bar{B}_r) \exp\left(-\frac{x}{b}\right), \quad (55)$$

207 where \bar{A}_0 and \bar{B}_0 represent the tidally averaged cross-sectional area and width at the
 208 estuary mouth, respectively, \bar{A}_r and \bar{B}_r represent the asymptotic riverine
 209 cross-sectional area and width, respectively, and a and b are the convergence lengths
 210 of the cross-sectional area and width, respectively. The advantage of these equations
 211 for approximating the shape of the estuary is that they account not only for the
 212 exponential shape in the lower part of the tidal river but also for the approximately
 213 prismatic channel in the upstream part of the tidal river. We further assume a nearly
 214 rectangular cross-section, considering a large width to depth ratio; hence, the tidally
 215 averaged depth is given by $\bar{h} = \bar{A}/\bar{B}$ and the cross-sectional area variability can be

设置了格式: 字体: (默认) Times New Roman
 设置了格式: 字体: (默认) Times New Roman
 设置了格式: 字体: (默认) Times New Roman

设置了格式: 字体: (默认) Times New Roman, 字体颜色: 文字 1
 设置了格式: 字体颜色: 文字 1, 检查拼写和语法
 设置了格式: 字体: (默认) Times New Roman, 字体颜色: 文字 1
 设置了格式: 字体: (默认) Times New Roman
 设置了格式: 字体: (默认) Times New Roman
 设置了格式: 字体: (默认) Times New Roman
 设置了格式: 字体: (默认) Times New Roman

设置了格式: 字体: (默认) Times New Roman
 设置了格式: 字体: (默认) Times New Roman
 设置了格式: 字体: (默认) Times New Roman
 设置了格式: 字体: (默认) Times New Roman
 设置了格式: 字体: (默认) Times New Roman
 设置了格式: 字体: (默认) Times New Roman

设置了格式: 字体: 非倾斜, 字体颜色: 文字 1, 英语(英国)

设置了格式: 字体颜色: 文字 1, 英语(英国)
 设置了格式: 字体颜色: 文字 1, 英语(英国)

216 primarily attributed to the change in depth. We further assume a nearly rectangular
217 cross section, considering the large width (2,000–910,000 km) relative to the small
218 depth (10–20 m) in the Yangtze estuary River channel; hence, the tidally averaged
219 depth is given by $\bar{h} = \bar{A}/\bar{B}$ and the cross-sectional area variability can be primarily
220 due attributed to the change in depth.

221 3.2.2 Analytical solution for tidal hydrodynamics

222 It was shown by Cai et al. (2014a, b, 2016) that the tide-river dynamics is dominantly
223 controlled by four dimensionless parameters (see their definitions in Table 1). They
224 include: the dimensionless tidal amplitude ζ (representing the boundary condition in
225 the seaward side), the estuary shape number γ (representing the cross-sectional area
226 convergence), the friction number χ (representing the bottom frictional effect), and the
227 dimensionless river discharge ϕ (representing the impact of freshwater discharge).

228 The definitions of these four variables are defined in Table 1, where η is the
229 tidal amplitude, v is the velocity amplitude, U_r is the river flow velocity, ω is the tidal
230 frequency, r_s is the storage width ratio accounting for the effect of storage area (i.e.
231 tidal flats or salt marshes), and c_0 is the classical wave celerity defined as

$$232 c_0 = \sqrt{gh/r_s}, \quad c_0 = \sqrt{gh/r_s}$$

233
234
235 where η is the tidal amplitude, v is the velocity amplitude, U_r is the river flow velocity,
236 ω is the tidal frequency, r_s is the storage width ratio accounting for the effect of
237 storage area (i.e. tidal flats or salt marshes), and c_0 is the classical wave celerity

- 设置了格式: 字体: 非倾斜, 字体颜色: 文字 1, 英语(英国)
- 设置了格式: 字体颜色: 文字 1, 英语(英国)
- 设置了格式: 字体: 非倾斜, 字体颜色: 文字 1, 英语(英国)
- 设置了格式: 字体颜色: 文字 1, 英语(英国)
- 设置了格式: 字体: 非倾斜, 字体颜色: 文字 1, 英语(英国)
- 设置了格式: 字体颜色: 文字 1, 英语(英国), 下标
- 设置了格式: 字体颜色: 文字 1, 英语(英国)
- 设置了格式: 字体: 非倾斜, 字体颜色: 文字 1, 英语(英国)
- 设置了格式: 字体颜色: 文字 1, 英语(英国)
- 设置了格式: 字体颜色: 文字 1, 英语(英国), 下标
- 设置了格式: 字体颜色: 文字 1, 英语(英国)
- 设置了格式: 字体颜色: 文字 1, 英语(英国), 下标
- 设置了格式: 字体: 倾斜
- 设置了格式: 字体: 非倾斜, 字体颜色: 文字 1, 英语(英国)
- 设置了格式: 字体颜色: 文字 1, 英语(英国)
- 设置了格式: 字体颜色: 文字 1, 英语(英国)
- 设置了格式: 字体颜色: 文字 1, 英语(英国)
- 设置了格式: 字体颜色: 文字 1, 英语(英国)
- 设置了格式: 字体颜色: 文字 1, 英语(英国)
- 设置了格式: 字体颜色: 文字 1, 英语(英国)
- 设置了格式: 字体颜色: 文字 1, 英语(英国)
- 设置了格式: 字体颜色: 文字 1, 英语(英国)
- 域代码已更改

238 defined as $c_0 = \sqrt{g\bar{h}/r_s}$.

239 Table 1. Definitions of dimensionless parameters used in the analytical model

Local variables	Dependent variables
Dimensionless tidal amplitude $\zeta = \eta / \bar{h}$	Amplification number $\delta = c_0 d\eta / (\eta \omega dx)$
Estuary shape number $\gamma = c_0 (\bar{A} - \bar{A}_r) / (\omega a \bar{A})$	Velocity number $\mu = v / (r_s \zeta c_0) = v \bar{h} / (r_s \eta c_0)$
Friction number $\chi = r_s g c_0 \zeta [1 - (4\zeta / 3)^2]^{-1} / (\omega K^2 \bar{h}^{4/3})$	Celerity number $\lambda = c_0 / c$
Dimensionless river discharge $\varphi = U_r / v$	Phase lag $\varepsilon = \pi / 2 - (\phi_z - \phi_v)$

240

241 In this study, we used the analytical solutions proposed by Cai et al. (2014a, b, 2016),
 242 in which the solutions of the major tide-river dynamics are derived by solving a set of
 243 four implicit equations for the tidal damping, the velocity amplitude, the wave celerity,
 244 and the phase lag (see details in Appendix B). The major dependent parameters can be
 245 described by the following four variables (see also Table 1): δ represents the
 246 damping/amplification number describing the increase ($\delta > 0$), or decrease ($\delta < 0$) of
 247 the tidal wave amplitude along the estuary axis, μ represents the velocity number
 248 indicating the ratio of actual velocity amplitude to the frictionless value in a prismatic
 249 channel, λ represents the celerity number representing the classical wave celerity c_0
 250 scaled by the actual wave celerity c , and ε represents the phase lag between the high

251 water (HW) and high water slack (HWS) or between the low water (LW) and low
252 water slack (LWS). It is important to note that the phase lag (ranging between 0 and
253 $\pi/2$) is a key parameter in classifying the estuary, where $\varepsilon = 0$ suggests the tidal wave
254 is featured by a standing wave, while $\varepsilon = \pi/2$ indicates a progressive wave. For a
255 simple harmonic wave, the phase lag is defined as $\varepsilon = \pi/2 - (\phi_z - \phi_v)$, where ϕ_z and
256 ϕ_v are the phases of elevation and current, respectively (Savenije, et al., 2008).

257

258 **3.2.3 Analytical solution for the entire channel**

259 It is worth noting that the analytically computed tide-river dynamics μ , δ , λ , and ε only
260 represent local hydrodynamics since they depend on local (fixed position) values of
261 the dimensionless parameters, i.e. the tidal amplitude ζ , the estuary shape number γ ,
262 the friction number χ , and the river discharge φ (see Table 1). To correctly reproduce
263 the tide-river dynamics for the entire channel, a multi-reach technique is adopted by
264 subdividing the entire estuary into multiple reaches to account for the longitudinal
265 variations of the estuarine sections (e.g. bed elevation, bottom friction). For a given
266 tidal damping/amplification number δ and tidal amplitude η at the seaward boundary,
267 it is possible to determine the tidal amplitude at a distance Δx (e.g. 1 km) upstream by
268 simple explicit integration. Hence, the analytical solution for the entire channel can be
269 obtained by step-wise integration in this way.

270

271 **4. Results**

272 **4.1 Observational analysis on the Alteration of the tide-river dynamics after**

设置了格式: 字体: 加粗

273 **TGD closure**

274 To quantify the impacts of TGD operation on the downstream tide-river dynamics, we
275 divided the time series into two periods, including a pre-TGD period (1979–1984,
276 representing the condition before the operation of the TGD) and a post-TGD period
277 (2003–2014, after the closure of the TGD with an operating TGD). Figure 2 shows the
278 changes in the observed tidal range ΔH and residual water level $\Delta \bar{Z}$ before and after
279 the closure of the TGD at the six gauging stations, together with the change in
280 freshwater discharge ΔQ observed at the DT hydrological station. Figure 2 and Table
281 2 clearly show that the monthly averaged river discharge in January, February, and
282 March substantially increased by 35.5%, 30.5%, and 16.4%, respectively, due to the
283 considerable release of freshwater from the TGD. On the other hand, we observe a
284 significant decrease in freshwater discharge in September, October, and November,
285 decreasing by 20.1%, 33.2%, and 20.8%, respectively. The reason can be primarily
286 attributed to the impounding water of the TGD during these months, especially in
287 October. During the other months, the impacts of TGD on the change in the
288 freshwater discharge are relatively small, mimicking the natural condition before the
289 operation of the TGD.

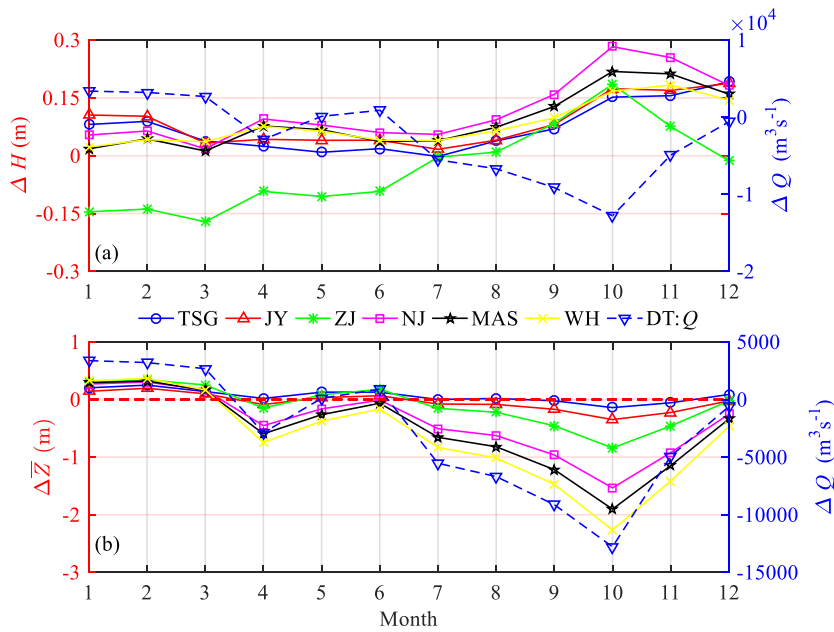
290

291 In Figure 2a we observe an increasing trend in tidal range for the post-TGD period at
292 the six gauging stations, except for the marked decrease at the ZJ station in the first
293 half of the year (i.e. January–June). On average, the maximum increase (0.20 m) in
294 tidal range occurs in October, which is mainly due to the substantial reduction of river

带格式的: 两端对齐

带格式的: 两端对齐

295 discharge caused by the TGD operation. This indicates a consistent enhancement of
 296 tidal dynamics along the Yangtze estuary, except the reach near the ZJ station. For the
 297 residual water level, Figure 2b clearly shows that the change in the residual water
 298 level directly follows that of the river discharge due to the stable relationship between
 299 these two parameters. In particular, we see that the residual water levels increased by
 300 0.26 m, 0.30 m, and 0.16 m, respectively, in January, February, and March, while they
 301 significantly decreased by 0.72 m, 1.17 m, and 0.70 m, respectively, in September,
 302 October, and November. In addition, the decrease trend in residual water level is more
 303 significant ~~in~~ at upstream stations when compared with those in the downstream
 304 areas.



305
 306 Figure 2. Changes in monthly averaged (a) tidal range ΔH and (b) residual water level
 307 $\Delta \bar{Z}$ together with the freshwater discharge ΔQ along the Yangtze River estuary.

308

309 Table 2. Comparison of multi-year monthly averaged river discharge Q ($\text{m}^3 \cdot \text{s}^{-1}$)

310 between the pre-TGD and the post-TGD periods

Month	1	2	3	4	5	6	7	8	9	10	11	12
Pre-TGD	9520	10527	16298	25050	30867	38283	49900	47276	45317	38467	23633	14810
Post-TGD	12896	13733	18974	22165	30971	39180	44367	40590	36187	25682	18714	14203
Change	3376	3206	2675	-2885	105	896	-5533	-6687	-9130	-12784	-4919	-607

311

312 Since the TGD operation affects tide-river dynamics primarily through the alteration
 313 of the freshwater discharge, it is worth exploring the patterns of trends in the
 314 relationship between the freshwater discharge and gradients of the main tidal
 315 parameters with respect to distance (i.e. the tidal damping rate and the residual water
 316 level slope). Here, we estimated the tidal damping rate δ_H and the residual water level
 317 slope S for a reach of Δx by using the following expressions:

318

$$\delta_H = \frac{1}{(H_1 + H_2)/2} \frac{H_2 - H_1}{\Delta x}, \quad (66)$$

319

$$S = \frac{\bar{Z}_2 - \bar{Z}_1}{\Delta x}, \quad (77)$$

320 where H_1 and \bar{Z}_1 are the tidal amplitude and residual water level on the seaward side,
 321 respectively, whereas H_2 and \bar{Z}_2 are the corresponding values Δx upstream,
 322 respectively. Figure 3 presents the computed tidal damping rates for different reaches
 323 along the Yangtze estuary based on the observed tidal ranges at the six gauging
 324 stations. It is remarkable that the tidal damping rates at the ZJ-NJ and MAS-WH
 325 reaches have significantly increased during the post-TGD period, which suggests an

设置了格式: 字体: 8 磅

设置了格式: 字体: 8 磅

设置了格式: 字体: 8 磅

设置了格式: 字体: 8 磅

设置了格式: 字体: (默认) Times New Roman

设置了格式: 字体: (默认) Times New Roman

设置了格式: 字体: (默认) Times New Roman

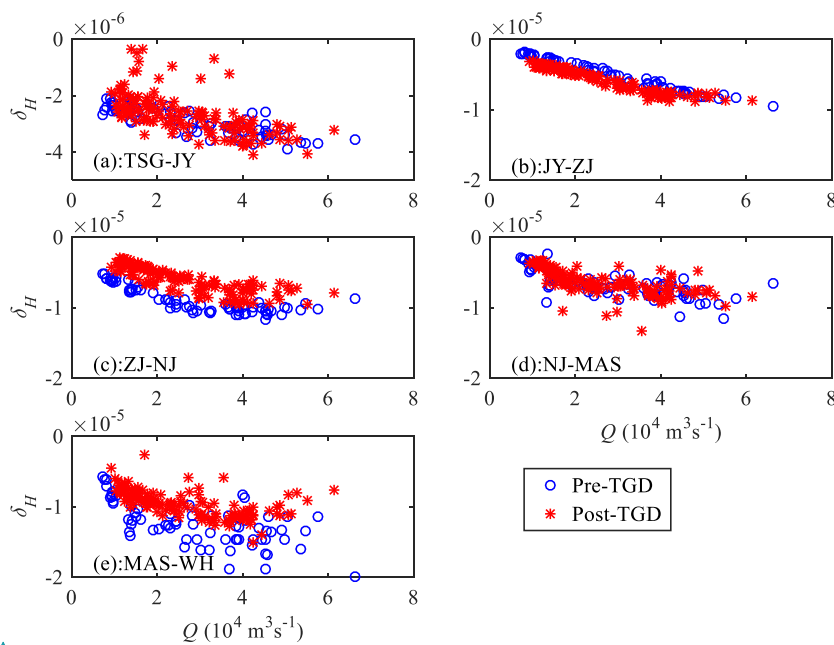
设置了格式: 字体: (默认) Times New Roman

设置了格式: 字体: (默认) Times New Roman

设置了格式: 字体: (默认) Times New Roman

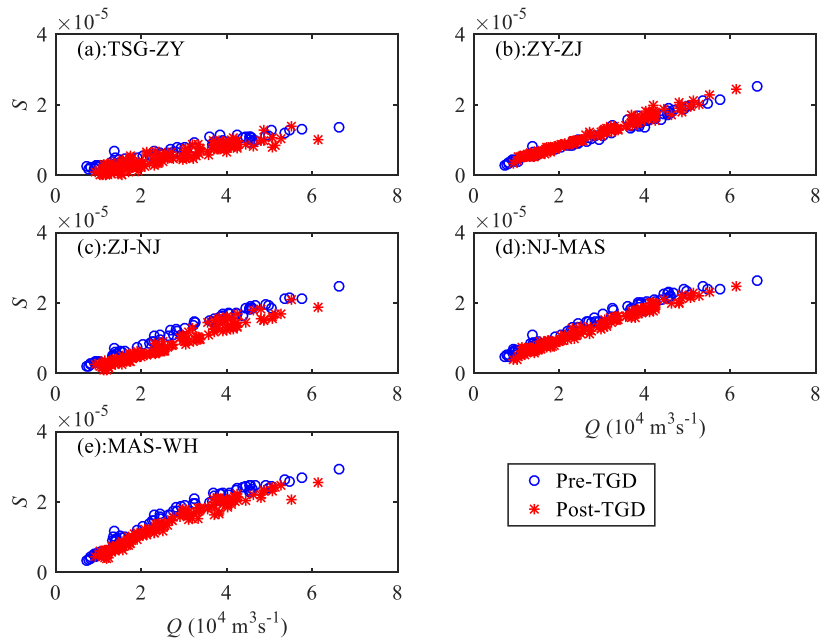
设置了格式: 字体: (默认) Times New Roman

326 enhancement of tidal dynamics under the current freshwater discharge conditions. On
 327 the contrary, a noticeable decrease in δ_H was observed at the JY-ZJ reach, which
 328 corresponds to a decrease in tidal range at the ZJ station for the low river discharge
 329 conditions (from January to May, see Figure 2a). At TGS-JY and NJ-MAS, no
 330 significant change in δ_H is observed. In Figure 4, a consistent decrease in the residual
 331 water level slope S is observed along the Yangtze estuary, except for the JY-ZJ reach.
 332 This means that the residual friction effect becomes weaker in the post-TGD period
 333 since the residual water level slope is primarily balanced by the residual friction term
 334 (Cai et al., 2014a, b, 2016).



335
 336 Figure 3. Changes in tidal damping rate δ_H before and after the TGD closure for
 337 different reaches along the Yangtze estuary: (a) TGS-JY, (b) JY-ZJ, (c) ZJ-NJ, (d)
 338 NJ-MAS, (e) MAS-WH.

设置了格式: 字体: (默认) Times New Roman, 小四, 字体
 颜色: 文字 1



设置了格式: 字体: (默认) Times New Roman, 小四, 字体颜色: 文字 1

339

340 Figure 4. Changes in residual water level slope S before and after the TGD closure for
 341 different reaches along the Yangtze estuary: (a) TGS-JY, (b) JY-ZJ, (c) ZJ-NJ, (d)
 342 NJ-MAS, (e) MAS-WH.

343

344 4.2 Performance of the analytical model reproducing the tide-river dynamics

345 The analytical model presented in Section 3.2 was subsequently applied to the
 346 Yangtze River estuary, with the seaward boundary using the tidal amplitude imposed
 347 at the TSG station and the landward boundary using the river discharge imposed at the
 348 DT station. The computation length of the estuary is 470 km, covering the entire
 349 estuary from TSG to DT. The adopted geometric characteristics (including the tidally
 350 averaged cross-sectional area, width, and depth) are the same for both pre- and
 351 post-TGD periods, which were extracted from a digital elevation model (DEM) using

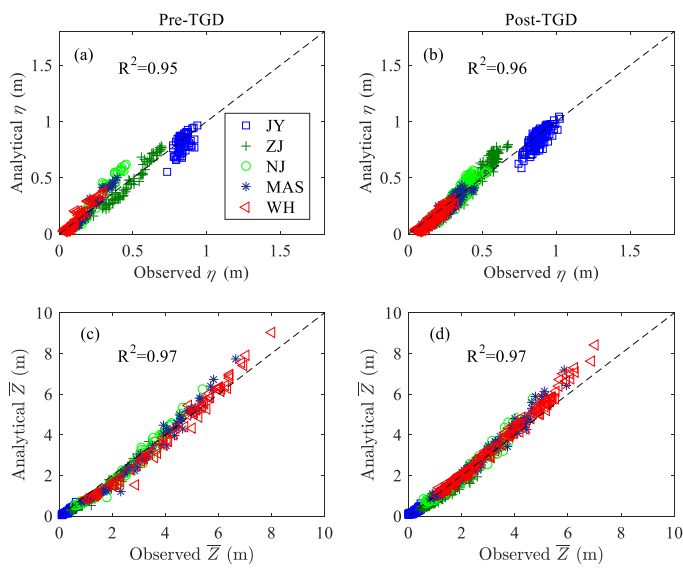
352 Yangtze River estuary navigation charts surveyed in 2007. The geometric
353 characteristics, calibrated by fitting the observed values using Equations (4) and (5),
354 are presented in Table 3, where a relatively large cross-sectional area convergence
355 length ($a = 151$ km) is evident, with a relatively small width ($b = 44$ km), indicating a
356 fast transition from a funnel-shaped reach to a prismatic reach in terms of width. It is
357 worth noting that the Yangtze River estuary is characterised by a typical semidiurnal
358 character; thus, a typical M_2 tidal period (i.e. 12.42 h) was adopted in the analytical
359 model. For the sake of simplification, we assume that the storage width ratio $r_S = 1$.
360 Hence, the only calibrated parameter is the Manning-Strickler friction coefficient K .
361 Here, we used two values for K : $K = 80 \text{ m}^{1/3} \cdot \text{s}^{-1}$ in the tide-dominated region ($x = 0$ –
362 42 km), and a smaller value of $K = 55 \text{ m}^{1/3} \cdot \text{s}^{-1}$ in the river-dominated region ($x = 42$ –
363 450 km). The analytically computed results were compared with the observed tidal
364 amplitudes and the residual water levels at five gauging stations along the Yangtze
365 estuary (Figure 5). It can be seen that the overall correspondence between analytical
366 results and observations is good, with high coefficients of determination ($R^2 > 0.95$),
367 which suggests the usefulness of the present analytical model for reproducing the
368 tide-river dynamics, given the gross features of flow characteristics and estuarine
369 geometry.

设置了格式: 字体颜色: 自动设置

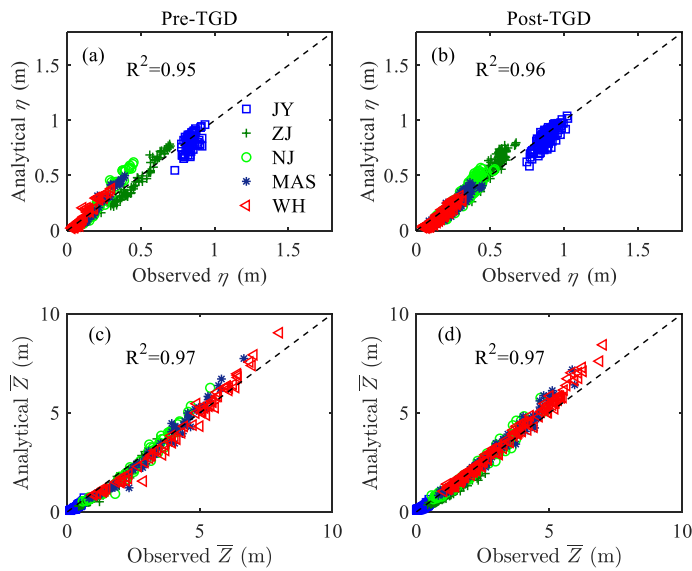
372
373 Table 3. Characteristics of geometric parameters in the Yangtze River estuary

Characteristics	River	Mouth	Convergence length a/b (km)
Cross-sectional area \bar{A} (m ²)	12,135	51,776	151
Width \bar{B} (m)	2005	6735	44

374



375



376

377 **Figure 5. Comparison of monthly mean averaged values for (a, b) Comparison of**
 378 **analytically computed tidal amplitude η and (c, d) residual water level \bar{Z} against the**
 379 **observations in the Yangtze River estuary for the pre-TGD period (1979–1984) and**
 380 **post-TGD period (2003–2014).**

381

382

383

384

385

386

387

388

389

- 设置了格式: 字体颜色: 自动设置
- 设置了格式: 字体颜色: 蓝色
- 设置了格式: 字体: (默认) Times New Roman, 小四, 英语 (英国)
- 设置了格式: 字体颜色: 自动设置
- 设置了格式: 字体颜色: 自动设置

390 **4.3 Impacts of TGD operation on spatial-temporal patterns of tide-river**
391 **dynamics**

392 With the significant seasonal discharge variations resulting from the TGD regulation,
393 an understanding of the seasonal impacts on tide-river dynamics along the estuary has
394 become increasingly important. In Figures 6 and 7, we see how the TGD operation
395 impacts the longitudinal variation of the main tidal dynamics in terms of the four
396 dependent parameters δ , λ , μ , and ε for different seasons. The most considerable
397 changes in the major tide-river dynamics occurred in both autumn and winter seasons,
398 which correspond to the substantial reduction in freshwater discharge in the
399 wet-to-dry transition period (i.e. autumn) and slightly increased freshwater discharge
400 in the dry season (i.e. winter) due to the TGD operation since 2003 (see Table 2). On
401 the other hand, the impacts of the TGD operation on the tide-river dynamics during
402 the spring and summer are relatively minor due to the negligible change in the
403 freshwater discharge. However, we do notice that the TGD had exerted slight
404 influence on tide-river dynamics in the downstream reaches ($x < 250$ km) during the
405 summer, with the maximum freshwater discharge occurring within a year. In addition,
406 it appears that there exists a critical position corresponding to the maximum tidal
407 damping (or minimum value of δ) upstream in which the tidal damping becomes weak.
408 This phenomenon occurs particularly in the spring, summer, and autumn. The
409 underlying mechanism is elaborated in the discussion section.

410

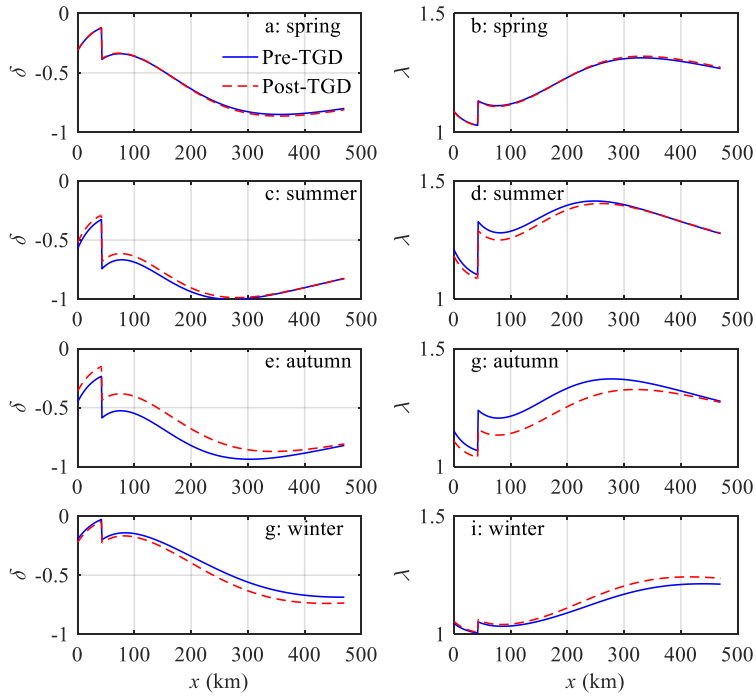
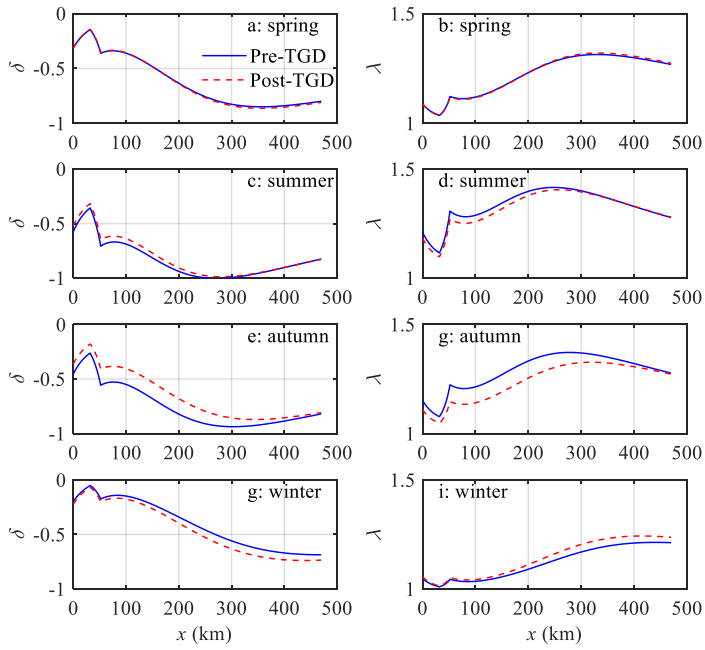
411 Figures 6a, c, e, g show the comparison of the analytically computed tidal damping

412 number δ before and after the closure of the TGD, in which we clearly ~~identify~~
413 ~~demonstrate~~ observe that the longitudinal tidal damping effect was considerably
414 weakened in autumn, while it was slightly enhanced in winter after the TGD closure.
415 This was expected since freshwater discharges tend to dampen the tidal wave
416 primarily through the enhancement of the friction term (Horrevoets et al., 2004; Cai et
417 al., 2014a, b, 2016). Figures 6b, d, g, i show a similar picture for the wave celerity
418 number λ , which is positively correlated to the tidal damping number δ , according to
419 the celerity equation (11) in Appendix B. Figure 7 shows the longitudinal computation
420 of the velocity number μ and the phase lag ε for both periods. The impacts of the TGD
421 operation on the velocity scale and phase lag are similar to the tidal damping, i.e. ~~the~~
422 ~~larger the freshwater discharge, the smaller the velocity number and the phase lag, the~~
423 ~~larger the freshwater discharge is, the smaller the velocity number and the phase lag~~
424 ~~are.~~

425
426 Overall, in the seaward reach of the estuary, the effect of freshwater discharge
427 alteration by the TGD operation on the major tide-river dynamics (i.e. δ , λ , μ , and ε)
428 was less significant because of the small ratio of freshwater discharge to tidal
429 discharge. On the other hand, in the upstream reach of the estuary, the changes in the
430 four dependent parameters are also small due to the substantial tidal attenuation as a
431 result of the long-distance propagation from the estuary mouth. Therefore, the pattern
432 of seasonal variation due to the TGD operation is relatively small at both ends of the
433 estuary, whereas the largest variation usually occurs in the middle reach of the estuary.

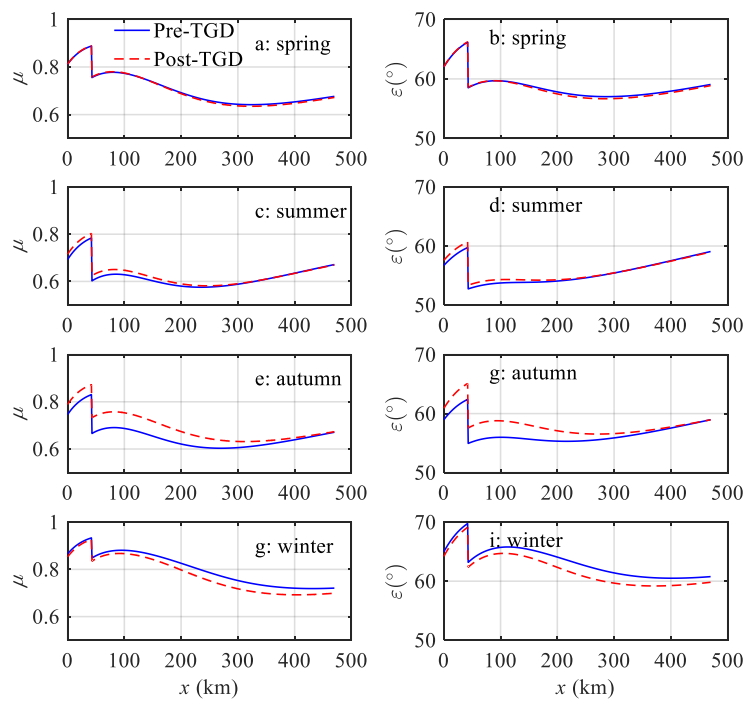
434 This finding was supported by the results of harmonic analysis using the numerical
435 results (Zhang et al., 2018). Similar phenomena have also been identified in other
436 large fluvial meso-tide estuaries, such as the Mekong River estuary and Amazon
437 River estuary, where dam operation altered the seasonal patterns of tide-river
438 dynamics (Kosuth et al., 2009; Hecht et al., 2018).

439



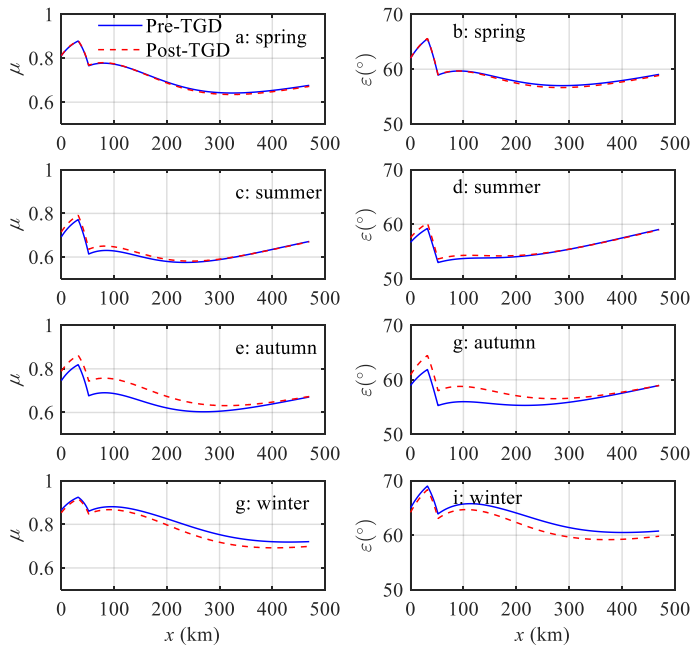
设置了格式: 字体: (默认) Times New Roman, 小四, 字体颜色: 文字 1

441 Figure 6. Longitudinal variability of simulated tidal damping number δ (a, c, e, g) and
442 celerity number λ (b, d, g, i) along the Yangtze estuary in different seasons (spring: a,
443 b; summer: c, d; autumn: e, g; winter: g, i) for both the pre-TGD and the post-TGD
444 periods.



445

设置了格式: 字体: (默认) Times New Roman, 小四, 字体颜色: 文字 1



446

447 Figure 7. Longitudinal variability of simulated velocity number μ (a, c, e, g) and phase
 448 lag ε (b, d, g, i) along the Yangtze estuary in different seasons (spring: a, b; summer: c,
 449 d; autumn: e, g; winter: g, i) for both the pre-TGD and the post-TGD periods.

450

451 5. Discussion

452 5.1 The impact of channel geometry alteration on tide-river dynamics

453 Dam operations, which dramatically modified downstream flow and sediment
 454 regimes, are becoming an increasingly important factor controlling the morphological
 455 evolution. Previous studies show that, as a result of the trapping of sediments by the
 456 TGD, considerable erosion occurred in the first several hundred km downstream of
 457 the TGD, considerably coarsening the bedload (Yang et al., 2014). In particular, [the](#)

458 ~~river bed immediately downstream was eroded~~~~the river immediately downstream~~
459 ~~eroded~~ at a rate of 65 Mt/yr in 2001–2002 (Yang et al., 2014). It was shown by Lyu et
460 al. (2018) that due to a dramatic reduction in the sediment discharge following the
461 construction of the TGD, a significant change in size, geometry, and spatial
462 distribution of pool-riffles occurred downstream; however, this adjustment was
463 limited to the reaches close to the TGD. It should be noted that the bathymetry
464 adopted in the analytical model is restricted to the estuarine area in 2007, which is
465 only 4 years after the TGD closure in 2003, and it is before the full operation of the
466 TGD began in 2009. In addition, the TGD is around 1600 km away from the estuary
467 mouth, and its influence on the estuarine morphology normally has a lag effect of at
468 least 4–5 years, as discussed by Wang et al. (2008). Hence, the adopted geometry has
469 been only partly altered after the TGD closure. The emorphological change of
470 Yangtze Estuary can be even more profound in recent years due to the continuously
471 and accumulated impact from the TGD. Further adjustment of morphological change
472 due to the sedimentation in the TGD could exert a considerable impact on the
473 tide-river dynamics in the estuarine region (e.g., Du et al., 2018; Shaikh et al., 2018).
474 Further study on the impact of morphological adjustment on the tide-river dynamics is
475 required in the future.
476 ~~Consequently, we concluded that the impact of the channel geometry alteration on~~
477 ~~tide river dynamics in the Yangtze River estuary is limited and, thus, the~~
478 ~~correspondence with the observed tidal amplitude and residual water level for the~~
479 ~~pre TGD period is good, such that we even used the geometry surveyed in 2007.~~

设置了格式: 字体: 非倾斜, 字体颜色: 文字 1, 英语(英国)

设置了格式: 字体: 非倾斜, 字体颜色: 文字 1, 英语(英国)

480

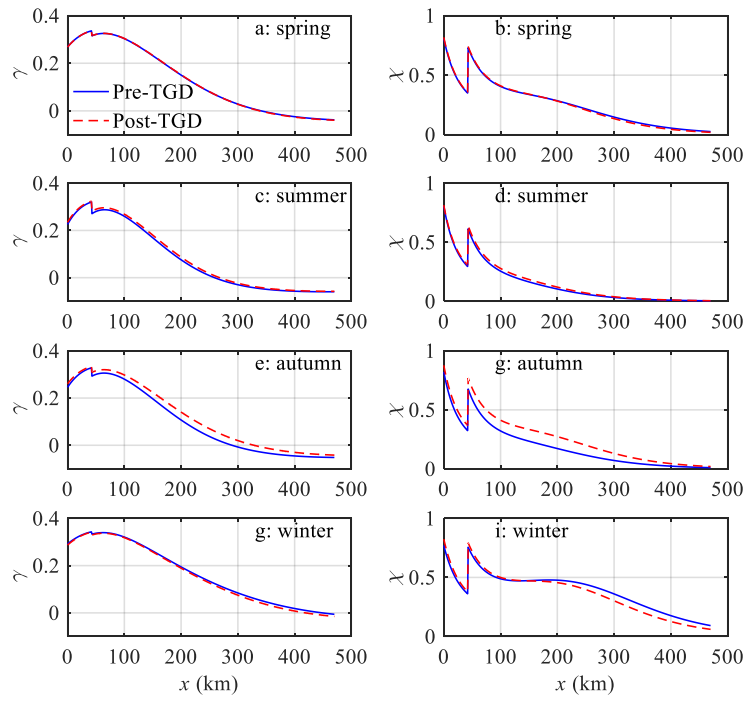
481 **5.2 The impact of freshwater discharge alteration on tide-river dynamics**

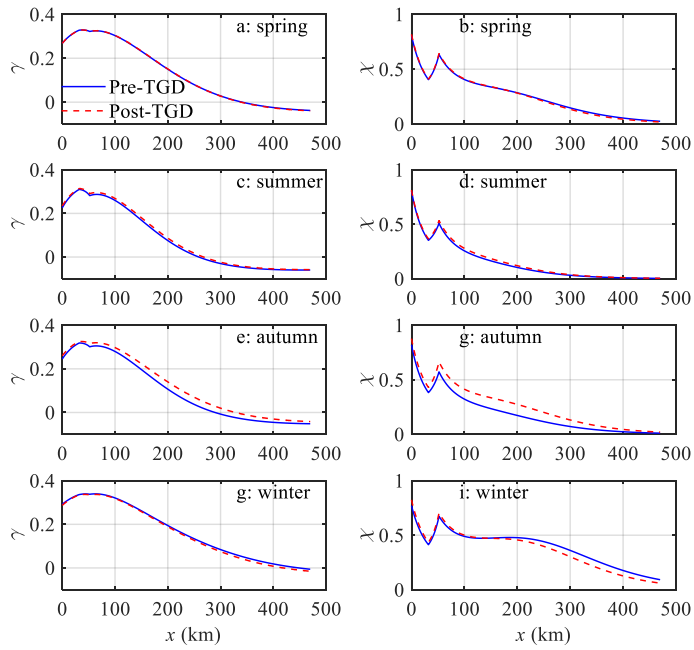
482

483 The water conservancy of the TGD has multiple purposes, in which the seasonal
484 discharge regulation and their impact on the ecosystem are well documented (e.g. Mei
485 et al., 2015a, b; Chen et al., 2016; Guo et al., 2018). However, the actual influence of
486 discharge regulation on the river-tide dynamics in the estuarine area is not fully
487 understood. With the analytical reproduction of tide-river dynamics for pre- and
488 post-TGD periods, it is possible to quantify the extent of the changes in the major
489 tidal dynamics, including the estuary shape number γ and friction number χ (Figure 8),
490 and the residual water level slope S and water depth h (Figure 9) along the Yangtze
491 River estuary. In general, during the transition from the wet season (summer–autumn)
492 to the dry season (winter–spring), the water level and corresponding fluvial discharge
493 downstream from the TGD is first raised by the impounding water and then reduced
494 by the release of water, which would substantially change the tide-river dynamics in
495 the downstream estuarine area, with the maximum variation occurring in autumn and
496 the minimum variation occurring in spring.

497

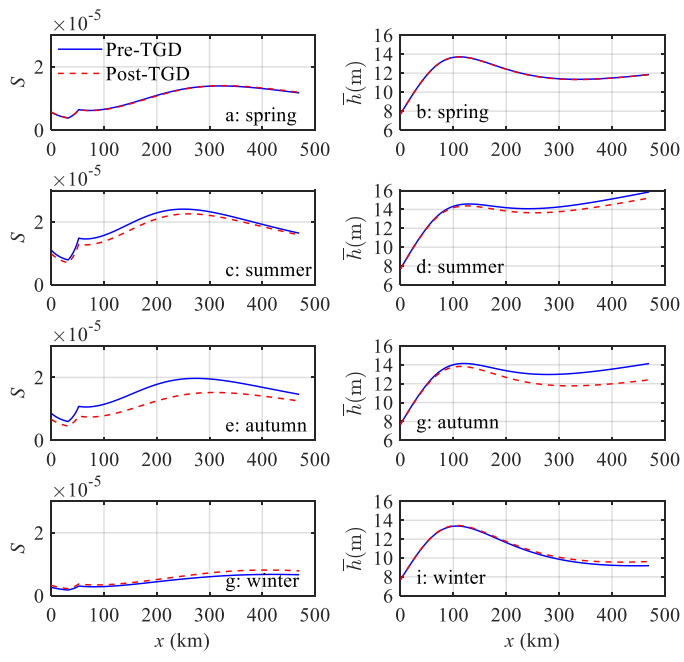
设置了格式: 字体: (默认) Times New Roman, 小四, 字体颜色: 文字 1



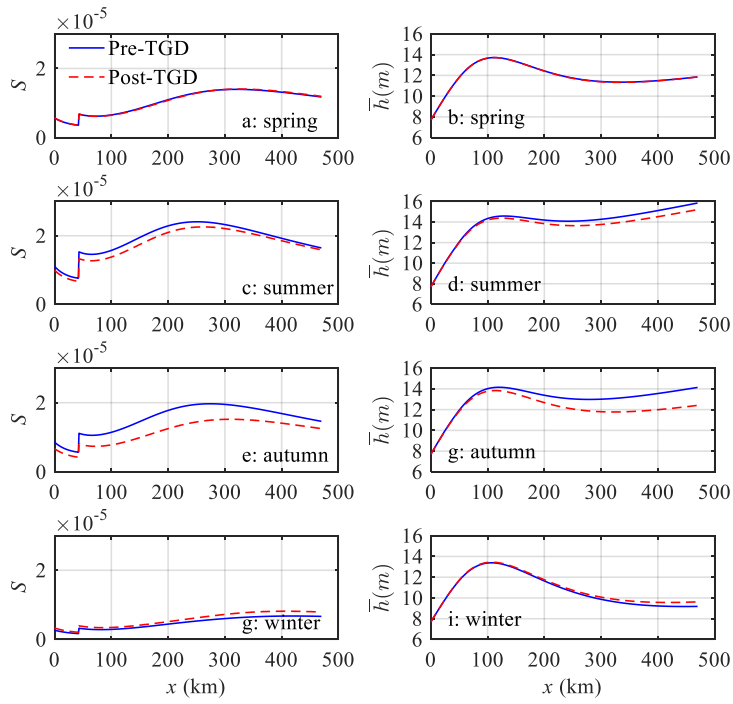


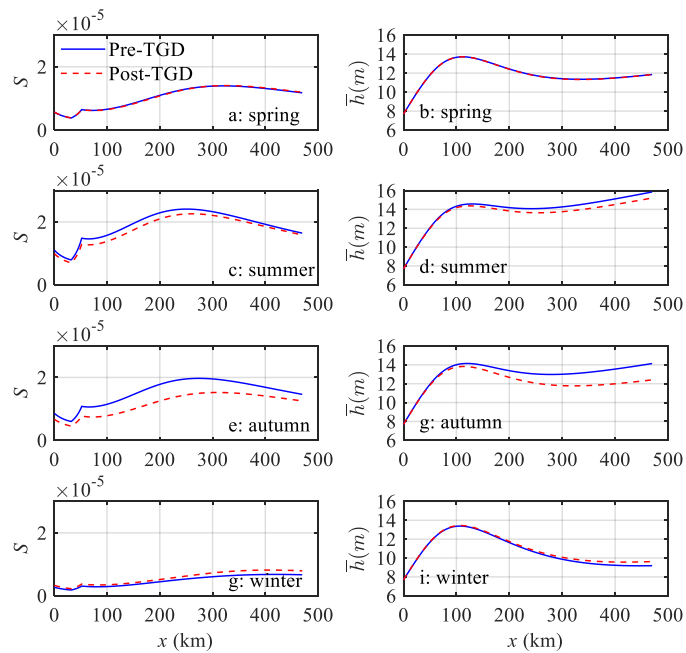
499

500 Figure 8. Longitudinal variability of simulated estuary shape number γ (a, c, e, g) and
 501 friction number χ (b, d, g, i) along the Yangtze estuary in different seasons (spring: a,
 502 b; summer: c, d; autumn: e, g; winter: g, i) for both the pre-TGD and the post-TGD
 503 periods.



设置了格式: 字体: (默认) Times New Roman, 小四, 字体颜色: 文字 1





506

507 Figure 9. Longitudinal variability of simulated residual water level slope S (a, c, e, g)
 508 and water depth h (b, d, g, i) along the Yangtze estuary in different seasons (spring: a,
 509 b; summer: c, d; autumn: e, g; winter: g, i) for both the pre-TGD and the post-TGD
 510 periods.

511

512 Figures 8 and 9 show that during the wet season (summer–autumn), the estuary shape
 513 number γ and friction number χ experience a general increase, while a decrease in the
 514 residual water level slope S and water depth \bar{h} can be identified in the post-TGD
 515 period due to the reduction in freshwater discharge. However, the changes in these
 516 major dynamics vary significantly along the channel. Near the estuary mouth, [where](#)
 517 [tidal influence overwhelms the influence from freshwater discharge](#) where the tidal

518 ~~influence dominates that of the freshwater discharge~~, the difference is relatively small,
519 as the magnitude of the freshwater discharge is small when compared with that of the
520 tidal discharge. Meanwhile at the upstream reach of the estuary, where the riverine
521 influence dominates that of the tide, the difference is also small due to the attenuation
522 of the tidal wave propagation over a long distance. Consequently, the most significant
523 changes in major tide-river dynamics occurred in the middle reach of the Yangtze
524 River estuary due to the discharge regulation of the TGD during the wet season. By
525 contrast, during the dry season (winter–spring), especially in winter, the opposite
526 trend was observed, indicating a slight increase in γ and χ , and a slight decrease in S
527 and \bar{h} due to the additional release of discharge from the TGD. In addition, we also
528 observed that the changes in tide-river dynamics caused by the TGD operation were
529 much stronger upstream than in the lower stream.

530

531 **5.3 Implications for water resource management**

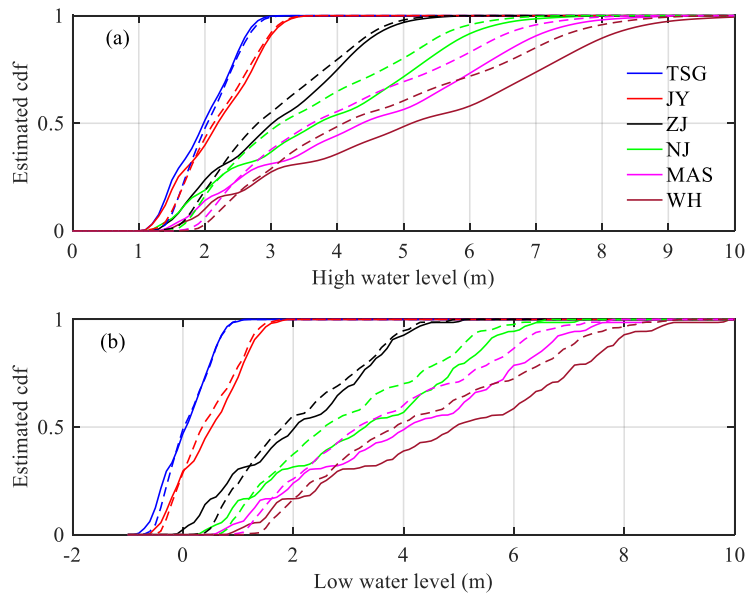
532 The construction of the TGD is the largest hydro-development project ever performed
533 in the world, having multiple influences on downstream water resource management,
534 including navigation, flood control, tidal limit variation, and salt intrusion.

535

536 **5.3.1 Implications for navigation**

537 The navigation condition is mainly controlled by both high water and low water levels.
538 Figure 10 shows the estimation of the cumulative distribution function (cdf) for both
539 the high-water level (Figure 10a) and the low-water level (Figure 10b) at the six

540 gauging stations along the Yangtze River estuary for both the pre- and post-TGD
541 periods. The results indicate that navigation conditions during the non-flood season
542 are generally improved, because both percentages of high-water and low-water levels
543 are increased due to the additional freshwater discharge released from the TGD. On
544 the other hand, during the flood season, the reduction in the freshwater discharge by
545 TGD impounding tends to exert a negative impact on navigation. However, the
546 reduced freshwater discharges in the late summer and autumn are not of sufficient
547 magnitude to cause any navigation problems. This is due to the fact that the mean
548 water levels during the flood season are relatively high; hence, the regulating flow
549 quantity and regulating capacity are relatively small (e.g. Chen et al., 2016). In
550 general, due to the staggered regulation in freshwater discharge, seasonally, the actual
551 navigation condition is improved due to the significant increase in the percentage of
552 low water levels.



553

554 Figure 10. Cumulative distribution function (cdf) estimated by using the kernel
 555 smoothing function (a) for high water level and (b) low water level at six gauging
 556 stations along the Yangtze estuary. The solid lines~~drawn lines~~ represent the pre-TGD
 557 period, while the dashed lines represent the post-TGD period.

558

559 5.3.2 Implications for flood control

560 Flood control is one of the most important functions of building dams and reservoirs
 561 in large rivers. Before the construction of the TGD, the Yangtze River basin suffered
 562 from frequent and disastrous flood threats. For instance, the floods of 1998 in the
 563 Yangtze River were reported to have killed 3656 people, destroyed 5.7 million homes,
 564 and damaged seven million more. Many studies have examined the flood control
 565 capacity of the TGD over the past two decades (Zhao et al., 2013; Chen et al., 2014).
 566 In particular, the capability of the TGD flood control is influenced by multiple factors

567 (e.g. Huang et al., 2018), particularly in the estuarine area, which is strongly
568 influenced by tides from the ocean. During the flood season, the reduced freshwater
569 discharge by TGD impounding benefits the flood control by reducing the peak flood
570 discharge. However, as the tidal influence is enhanced, both the percentages of high
571 water and low water levels for the post-TGD period are considerably increased, as
572 shown in Figure 10, indicating a decreased flood control capability. For instance, at
573 the WH gauging station located in the upstream part of the Yangtze River estuary, the
574 8-m high-water level increased by approximately 10% after the TGD closure during
575 the wet season. The corresponding flood prevention standard, therefore, is reduced
576 due to the increased high-water level (see also Nakayama and Shankman, 2013).
577 ~~The corresponding flood prevention standard, therefore, is reduced from the 20-year~~
578 ~~return period to the 10-year return period due to the increased high-water level.~~

设置了格式: 字体: 非倾斜, 字体颜色: 文字 1, 英语(英国)

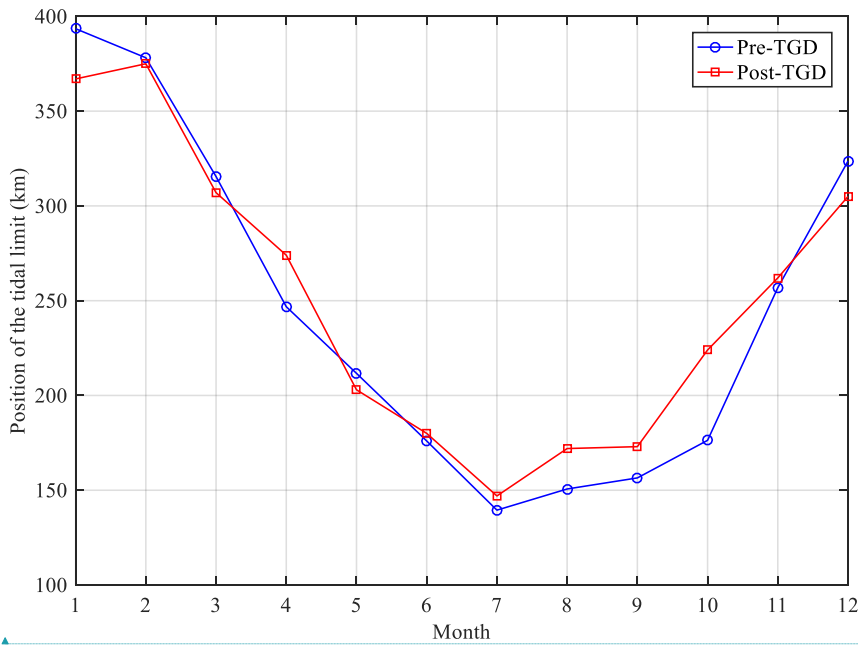
579 **5.3.3 Implications for tidal limit**

580 It is important to detect the position of the tidal limit (corresponding with the position
581 where the tidal amplitude to depth ratio is less than a certain threshold, e.g. $\frac{\eta}{h} < 0.02$),
582 which is the farthest point upstream where a river is affected by tidal fluctuations,
583 since it is essential for surveying, navigation, and fisheries management, in general
584 (e.g. Shi et al., 2018). Subsequently, we are able to define the tide-influenced length
585 as the distance upstream from the estuary mouth to the tidal limit. Generally, the tidal
586 limit fluctuates with the changes in the seasonal freshwater discharges. Field
587 measurements have demonstrated that tidal limit can reach as far as the NJ station and
588 further upstream during the dry season, while during the wet season, it is pushed
589 down to the ZJ station and may be pushed further downward to the JY station under

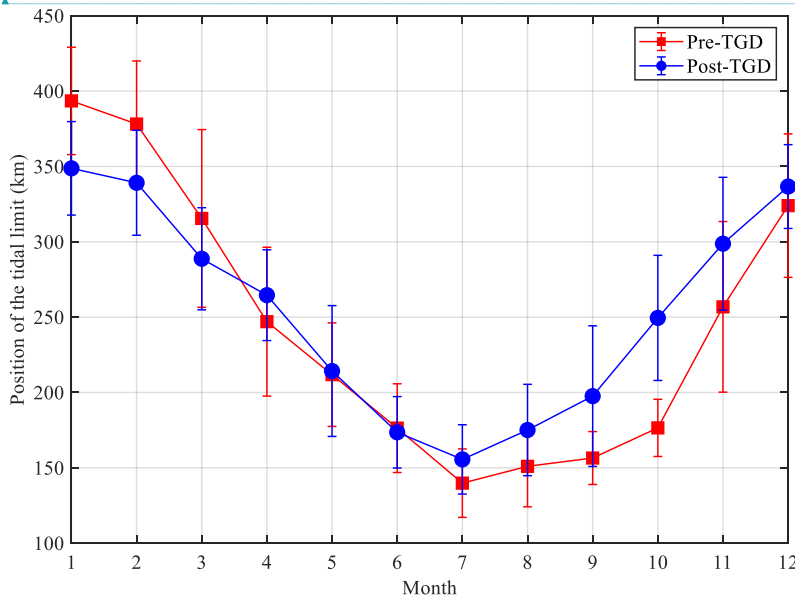
590 spate conditions. Figure 11 shows the analytically computed tidal limit position for
591 both the pre- and post-TGD periods. It can be observed that the tidal limit moved
592 downstream by about ~~25~~45 km and ~~250~~39 km in January and ~~December~~February
593 under the impact of the additional release of discharge from TGD during the dry
594 season. During the transition from dry to wet seasons (January–May), the total
595 freshwater discharge from TGD increases, and we identify further downstream
596 movement of the tidal limit, although to a smaller extent. The reverse of the post-TGD
597 tidal limit in April is due to the decrease in the freshwater discharge compared with
598 the pre-TGD tidal limit (see Table 2). The TGD storage period begins in June, and the
599 tidal limit moved upstream by a large amount compared with the pre-TGD period.
600 The largest change occurred during October when the tidal limit moved from 175 km
601 pre-TGD to ~~250~~25 km post-TGD due to the substantial increase in freshwater
602 discharge (see Table 2).

603

604



设置了格式: 字体: (默认) Times New Roman, 小四, 字体颜色: 文字 1



605

606

607 Figure 11. Temporal variation of the position of the tidal limit relative to the TSG
 608 station for both the pre-TGD and the post-TGD periods. [The vertical error bar at each](#)

609 [data point indicates the standard deviation of the analytically computed time series.](#)

610

611 **5.3.4 Implications for salt intrusion**

612 The operation of the TGD changed the location of tidal limit, which, in turn, directly
613 influences the intensity of saltwater intrusion, especially during the dry season, when
614 the freshwater discharge is low and saltwater intrusion is important (e.g. Cai et al.,
615 2015). The analysis of tide-river dynamics shows that the tidal dynamics are
616 considerably enhanced during the autumn due to the substantial decline in freshwater
617 discharged into the estuary, which may lead to enhanced saltwater intrusion. However,
618 with supplemented discharge after the TGD during the winter, saltwater intrusion
619 tends to be significantly suppressed, and the isohalines are pushed seaward by
620 additional river discharges (e.g. An et al., 2009; Qiu and Zhu, 2013). In contrast,
621 during the wet season, the TGD operation slightly extended the timing of saltwater
622 intrusion and increased its intensity by impounding freshwater. Since the total river
623 discharge rate during the wet season is the largest during the year, the influence of
624 saltwater on freshwater reservoirs along the coastal area is limited. Therefore, the
625 operation of TGD is overall favourable for reducing the burden of freshwater
626 supplement in the tidally influenced estuarine areas. [However, to quantify the](#)

627 [potential impacts of TGD's operation on salt intrusion and related aquatic ecosystem](#)

628 [health in general, it is required to couple the hydrodynamic model to the ecological or](#)

629 [salt intrusion model \(e.g., Qiu and Zhu, 2013; Cai et al., 2015\).](#)

630

设置了格式: 字体: 非倾斜

设置了格式: 字体: 非倾斜

631 **6. Conclusions**

632 An analytical approach was used to examine the potential impacts of TGD operation
633 on the spatial-temporal patterns of tide-river dynamics along the Yangtze River
634 estuary. It was shown that the freshwater regulation caused by the TGD, on a seasonal
635 scale, exerts significant impacts on the tide-river dynamics, with the maximum
636 influence occurring in autumn and winter. This generally corresponds to a dramatic
637 decrease in freshwater discharge during the wet-to-dry transition period and a slight
638 increase in discharge during the dry season. The analytical results indicate that the
639 discharge regulation by the TGD drives the alterations in the tide-river dynamics
640 instead of the geometric change. In particular, the change in the freshwater discharge
641 changes the estuary shape number (representing the geometric effect), the residual
642 water level slope (representing the effective frictional effect) and, hence, the tide-river
643 dynamics. This study, using the Yangtze River estuary ~~as an example as a significant~~
644 ~~ease study~~, provides an effective yet simple method to quantify the seasonal regulation
645 in freshwater discharge by large reservoirs or dams on hydrodynamics in estuaries.
646 The results obtained from this study will, hopefully, shed new light on aspects of
647 water resource management, such as navigation, flood control, and salt intrusion.

648

649 **Data availability.** Data and results are available from the authors upon request.

650

651 **Author contributions.** All authors contributed to the design and development of the
652 work. The experiments were originally carried out by Huayang Cai, Xianyi Zhang and

设置了格式: 字体: 加粗, 字体颜色: 自动设置, 英语(美国)

设置了格式: 字体: 加粗, 字体颜色: 自动设置, 英语(美国)

653 [Leicheng Guo carried out the data analysis. Min Zhang built the model and wrote the](#)
654 [paper. Feng Liu and Qingshu Yang reviewed the paper.](#)

设置了格式: 字体: (默认) Times New Roman, 小四, 字体颜色: 文字 1, 英语(英国)

设置了格式: 字体: (默认) Times New Roman, 小四, 字体颜色: 文字 1, 英语(英国)

655 [Competing interests. The authors declare that they have no conflict of interest.](#)

设置了格式: 字体: 加粗, 字体颜色: 自动设置, 英语(美国)

656 **Acknowledgments.**

设置了格式: 字体: 非加粗, 字体颜色: 文字 1, 英语(英国)

657 We acknowledge the financial support from the [National Key R&D of China \(Grant](#)
658 [No. 2016YFC0402600\)](#), from the Open Research Fund of State Key Laboratory of
659 Estuarine and Coastal Research (Grant No. SKLEC-KF201809), from the National
660 Natural Science Foundation of China (Grant No. 51709287 and 41701001), ~~from the~~
661 ~~[Basic Research Program of Sun Yat Sen University \(Grant No. 17lgzd12\)](#)~~, and from
662 the Guangdong Provincial Natural Science Foundation of China (Grant No.
663 2017A030310321).

设置了格式: 字体颜色: 文字 1, 英语(英国)

设置了格式: 字体颜色: 文字 1, 英语(英国)

666 **References**

667 An, Q., Wu., Y., and Taylor, S.: Influence of the Three Gorges Project on saltwater
668 intrusion in the Yangtze River Estuary, Environ. Geol., 56, 1679-1686,
669 <https://doi.org/10.1007/s00254-008-1266-4>, 2009.

670 Alebregtse, N. C., and de Swart, H. E.: Effect of river discharge and geometry on
671 tides and net water transport in an estuarine network, an idealized model applied to
672 the Yangtze estuary, Cont. Shelf. Res., 123, 29-49,
673 <https://doi.org/10.1016/j.csr.2016.03.028>, 2016.

674 Buschman, F. A., Hoitink, A. J. F., van der Vegt, M., and Hoekstra, P.: Subtidal water

675 level variation controlled by river flow and tides, *Water Resour. Res.*, 45(10), W10420,
676 <https://doi.org/10.1029/2009WR008167>, 2009.

677 Cai, H., Savenije, H. H. G., and Toffolon, M.: Linking the river to the estuary,
678 influence of river discharge on tidal damping, *Hydrol. Earth Syst. Sci.*, 18(1), 287-304,
679 <https://doi.org/10.5194/hess-18-287-2014>, 2014a.

680 Cai, H., Savenije, H. H. G., and Jiang, C.: Analytical approach for predicting fresh
681 water discharge in an estuary based on tidal water level observations, *Hydrol. Earth*
682 *Syst. Sci.*, 18(10), 4153-4168, <https://doi.org/10.5194/hess-18-4153-2014>, 2014b.

683 Cai, H., Savenije, H.H.G., Zuo, S., Jiang, C., and Chua, V.: A predictive model for salt
684 intrusion in estuaries applied to the Yangtze estuary, *J. Hydrol.*, 529, 1336-1349,
685 <https://doi.org/10.1016/j.jhydrol.2015.08.050>, 2015.

686 [Cai, H., Savenije, H. H. G., Jiang, C. Zhao L., Yang Q.: Analytical approach for](#)
687 [determining the mean water level profile in an estuary with substantial fresh water](#)
688 [discharge, *Hydrol. Earth Syst. Sci.*, 20, 1-19, <https://doi.org/10.5194/hess-20-1-2016>,](#)
689 [2016.](#)

690 Chen, J., Finlayson, B.L., Wei, T., Sun, Q., Webber, M., Li, M., and Chen, Z.:
691 Changes in monthly flows in the Yangtze River, China-With special reference to the
692 Three Gorges Dam, *J. Hydrol.*, 536, 293-301,
693 <https://doi.org/10.1016/j.jhydrol.2016.03.008>, 2016.

694 Chen, J., Zhong, P.A., Zhao, Y.F.: Research on a layered coupling optimal operation
695 model of the Three Gorges and Gezhouba cascade hydropower stations, *Energy*
696 *Convers. Manage.* 86 (5), 756-763, <https://doi.org/10.1016/j.enconman.2014.06.043>,

697 2014.

698 Dai, M., Wang, J., Zhang, M., and Chen, X.: Impact of the Three Gorges Project
699 operation on the water exchange between Dongting Lake and the Yangtze River, *Int. J.*
700 *Sediment Res.*, 32, 506-514, <https://doi.org/10.1016/j.ijsrc.2017.02.006>, 2017.

701 Dronkers, J. J.: *Tidal Computations in River and Coastal Waters*, Elsevier, New York,
702 USA, <https://doi.org/10.1126/science.146.3642.390>, 1964.

703 [Du, J., Shen, J., Zhang, Y.J., Ye, F., Liu, Z., Wang, Z., Wang, Y.P., Yu, X., Sisson, M.,
704 Wang, H.V.: 2018. Tidal Response to Sea-Level Rise in Different Types of Estuaries:
705 The Importance of Length, Bathymetry, and Geometry, *Geophys Res Lett.*, 45\(1\),
706 227-235, <https://doi.org/10.1002/2017GL075963>, 2018.](#)

707 Friedrichs, C. T., and Aubrey, D. G.: Non-linear tidal distortion in shallow well-mixed
708 estuaries, A synthesis, *Estuar. Coast. Shelf S.*, 27, 521-545,
709 [https://doi.org/10.1016/0272-7714\(88\)90082-0](https://doi.org/10.1016/0272-7714(88)90082-0), 1988.

710 Guo, L., van der Wegen, M., Jay, D.A., Matte, P., Wang, Z.B., Roelvink, D.J.A., He,
711 Q.: River-tide dynamics, Exploration of nonstationary and nonlinear tidal behavior in
712 the Yangtze River estuary, *J. Geophys. Res.*, 120(5), 3499-3521,
713 <https://doi.org/10.1002/2014JC010491>, 2015.

714 Guo, L., Su, N., Zhu, C., and He, Q.: How have the river discharges and sediment
715 loads changed in the Changjiang River basin downstream of the Three Gorges Dam? *J.*
716 *Hydrol.*, 560, 259-274, <https://doi.org/10.1016/j.jhydrol.2018.03.035>, 2018.

717 Hoitink, A. J. F., and Jay, D. A.: Tidal river dynamics: implications for deltas, *Rev.*
718 *Geophys.*, 54, 240-272, <https://doi.org/10.1002/2015RG000507>, 2016.

719 Hoitink, A. J. F., Wang, Z. B., Vermeulen, B., Huismans, Y., and Kastner, K.: Tidal
720 controls on river delta morphology, *Nat. Geosci.*, [https://doi.org/10,](https://doi.org/10.1038/ngeo3000)
721 [10.1038/ngeo3000](https://doi.org/10.1038/ngeo3000), 2017.

722 Horrevoets, A. C., Savenije, H. H. G., Schuurman, J. N., and Graas, S.: The influence
723 of river discharge on tidal damping in alluvial estuaries, *J. Hydrol.*, 294, 213-228,
724 <https://doi.org/10.1016/j.jhydrol.2004.02.012>, 2004.

725 Hecht, J.S., Lacombe, G., Arias, M.E., Duc Dang, T. and Piman, T.: Hydropower
726 dams of the Mekong River basin, a review of their hydrological impacts, *J. Hydrol.*,
727 45(10): W10420, <https://doi.org/10.1016/j.jhydrol.2018.10.045>, 2018.

728 Huang, K., Ye, L., Chen, L., Wang, Q., Dai, L., Zhou, J., Singh, V. P., Huang, M., and
729 Zhang, J.: Risk analysis of flood control reservoir operation considering multiple
730 uncertainties, *J. Hydrol.*, 565, 672-684, <https://doi.org/10.1016/j.jhydrol.2018.08.040>,
731 2018.

732 Kuang, C., Chen, W., Gu, J., Su, T. C., Song, H., Ma, Y., and Dong, Z.: River
733 discharge contribution to sea-level rise in the Yangtze River Estuary, China, *Cont.*
734 *Shelf. Res.*, 134, 63-75, <https://doi.org/10.1016/j.csr.2017.01.004>, 2017.

735 Kosuth, P., Callède, J., Laraque, A., Filizola, N., Guyot, J.L., Seyler, P., Fritsch, J.M.,
736 and Guimarães, V.: Sea-tide effects on flows in the lower reaches of the Amazon
737 River, *Hydrol. Process.*, 23(22), 3141-3150, <https://doi.org/10.1002/hyp.7387>, 2009.

738 [Liu, F., Hu, S., Guo, X., Cai, H., Yang, Q.: Recent changes in the sediment regime of](#)
739 [the Pearl River \(South China\), Causes and implications for the Pearl River Delta,](#)
740 [Hydrol. Process., 32\(12\): 1771-1785, https://doi.org/10.1002/hyp.11513, 2018.](#)

741

742 Lu, S., Tong, C., Lee, D.Y., Zheng, J., Shen, J., Zhang, W., and Yan, Y.: Propagation
743 of tidal waves up in Yangtze Estuary during the dry season, *J. Geophys. Res.*,
744 ~~120(9):~~, 6445-6473, <https://doi.org/10.1002/2014JC010414>, 2015.

745 Lu, X.X., Yang, X., and Li, S.: Dam not sole cause of Chinese drought, *Nature*
746 ~~475(7355):~~, 174, <https://doi.org/10.1038/475174c>, 2011.

747 Lyu, Y., Zheng, S., Tan, G. and Shu, C.: Effects of Three Gorges Dam operation on
748 spatial distribution and evolution of channel thalweg in the Yichang-Chenglingji
749 Reach of the Middle Yangtze River, China, *J. Hydrol.*, 565, 429-442,
750 <https://doi.org/10.1016/j.jhydrol.2018.08.042>, 2018.

751 Mei, X., Dai, Z., Gelder, P.H.A.J. and Gao, J.: Linking Three Gorges Dam and
752 downstream hydrological regimes along the Yangtze River, China, *Earth Space Sci.*,
753 2(4), 94-106, <https://doi.org/10.1002/2014EA000052>, 2015a.

754 Mei, X., Dai, Z., Du, J. and Chen, J.: Linkage between Three Gorges Dam impacts
755 and the dramatic recessions in China's largest freshwater lake, Poyang Lake, *Sci. Rep.*,
756 5,18197, <https://doi.org/10.1038/srep18127>, 2015b.

757 ~~[Nakayama, T., and Shankman, D.: 2013, Impact of the Three-Gorges Dam and water](#)~~
758 ~~[transfer project on Changjiang floods, Global Planet Change](#)~~
759 ~~[and Planetary Change, 100, 38–50, https://doi.org/doi:](#)~~
760 ~~[10.1016/j.gloplacha.2012.10.004, 2012-10-004, 2013.](#)~~

761 ~~Liu, F., Hu, S., Guo, X., Cai, H., Yang, Q.: Recent changes in the sediment regime of~~
762 ~~the Pearl River (South China), Causes and implications for the Pearl River Delta,~~

763 ~~Hydrol. Process., 32(12): 1771-1785, <https://doi.org/10.1002/hyp.11513>, 2018.~~
764 Qiu, C. and Zhu., J.: Influence of seasonal runoff regulation by the Three Gorges
765 Reservoir on saltwater intrusion in the Changjiang River Estuary, Cont. Shelf Res., 71,
766 16-26, <https://doi.org/10.1016/j.csr.2013.09.024>, 2013.
767 Rahman, M., Dustegir, M., Karim, R., Haque, A., Nicholls, R. J., Darby, S. E.,
768 Nakagawa, H., Hossain, M., Dunn, F. E., and Akter, M.: Recent sediment flux to the
769 Ganges-Brahmaputra-Meghna delta system, Sci. Total Environ., 643, 1054-1064,
770 <https://doi.org/10.1016/j.scitotenv.2018.06.147>, 2018.
771 Räsänen, T. A., Someth, P., Lauri, H., Koponen, J., Sarkkula, J., and Kummu, M.:
772 Observed river discharge changes due to hydropower operations in the Upper Mekong
773 Basin, J. Hydrol., 545, 28-41, <https://doi.org/10.1016/j.jhydrol.2016.12.023>, 2017.
774 Sassi, M. G., and Hoitink, A. J. F.: River flow controls on tides and tide-mean water
775 level profiles in a tidal freshwater river, J. Geophys. Res., 118(9), 4139-4151,
776 <https://doi.org/10.1002/jgrc.20297>, 2013.
777 Savenije, H. H. G.: Salinity and Tides in Alluvial Estuaries, Elsevier, New York, USA,
778 2005.
779 Savenije, H. H. G.: Salinity and Tides in Alluvial Estuaries (2nd completely revised
780 edition), Available at www.salinityandtides.com (Last access: 10 December 2018),
781 2012.
782 Savenije, H. H. G., Toffolon, M., Haas, J., and Veling, E. J. M.: Analytical description
783 of tidal dynamics in convergent estuaries, J. Geophys. Res., 113, C10025,
784 <https://doi.org/10.1029/2007JC004408>, 2008.

785 Shaikh, B.Y., Bansal, R.K., Das, S.K.: 2018. Propagation of Tidal Wave in Coastal
786 Terrains with Complex Bed Geometry. Environmental Processes, 5(3): 519-537.
787 <https://doi.org/10.1007/s40710-018-0314-7>, 2018.

788 Shi, S., Cheng, H., Xuan, X., Hu, F., Yuan, X., Jiang, Y., and Zhou, Q.: Fluctuations in
789 the tidal limit of the Yangtze River estuary in the last decade, Sci. China Earth
790 Sci., 61 (8): 1136-1147, <https://doi.org/10.1007/s11430-017-9200-4>, 2018.

791 Wang, Y., Ridd, P.V., Wu, H., Wu, J. and Shen, H.: Long-term morphodynamic
792 evolution and the equilibrium mechanism of a flood channel in the Yangtze Estuary
793 (China), Geomorphology, 99(1-4), 130-138,
794 <https://doi.org/10.1016/j.geomorph.2007.10.003>, 2008.

795 Vignoli, G., Toffolon, M., and Tubino, M.: Non-linear frictional residual effects on
796 tide propagation, in, Proceedings of XXX IAHR Congress, vol. A, 24-29 August 2003,
797 Thessaloniki, Greece, 291-298, 2003.

798 Zhang, E. F., Savenije, H. H. G., Chen, S. L., and Mao, X. H.: An analytical solution
799 for tidal propagation in the Yangtze Estuary, China, Hydrol. Earth Syst. Sci., 16(9),
800 3327-3339, <https://doi.org/10.5194/hess-16-3327-2012>, 2012.

801 Zhang, F., Sun, J., Lin, B., and Huang, G.: Seasonal hydrodynamic interactions
802 between tidal waves and river flows in the Yangtze Estuary, J. Marine Syst., 186,
803 17-28, <https://doi.org/10.1016/j.jmarsys.2018.05.005>, 2018.

804 Zhang, M., Townend, I., Cai, H., and Zhou, Y.: Seasonal variation of tidal prism and
805 energy in the Changjiang River estuary: A numerical study, Chin. J. Oceanol. Limn.,
806 34 (1), 219-230, <https://doi.org/10.1007/s00343-015-4302-8>, 2015a.

设置了格式: 字体颜色: 自动设置

设置了格式: 字体颜色: 自动设置

设置了格式: 字体颜色: 自动设置

设置了格式: 字体颜色: 自动设置

设置了格式: 字体颜色: 自动设置

807 Zhang, M., Townend, I., Cai, H., and Zhou, Y.: Seasonal variation of river and tide
 808 energy in the Yangtze estuary, China, Earth Surf. Proc. Land., 41(1): 98-116,
 809 <https://doi.org/10.1002/esp.3790>, 2015b.

810 Zhao, T., Zhao, J., Yang, D. and Wang, H.: Generalized martingale model of the
 811 uncertainty evolution of streamflow forecasts, Adv. Water Resour., 57, 41-51,
 812 <https://doi.org/10.1016/j.advwatres.2013.03.008>, 2013.

813

814 **Appendix A. Simplified momentum balance for the residual water level slope**

815 Assuming a periodic variation of flow velocity, the integration of Equation (1)(4) over
 816 a tidal cycle leads to an expression for the residual water level slope (e.g. Cai et al.,
 817 2014a, 2016):

818
$$\frac{\partial \bar{Z}}{\partial x} = -\frac{1}{K^2} \left(\frac{\overline{|U|U|}}{h^{4/3}} \right) - \frac{1}{2g} \frac{\partial \overline{U^2}}{\partial x} - \frac{1}{2\rho_0} h \frac{\partial \overline{\rho}}{\partial x} \quad (88)$$

819 where the overbars and the subscript 0 indicate the tidal average and value at the
 820 seaward boundary, respectively. The residual water level slope is induced by three
 821 contributions: residual frictional, advective acceleration, and density effects, which
 822 correspond to the three terms on the right-hand side of Equation (8)(8). Note that the
 823 contribution from advective acceleration to the residual water level slope:

824
$$\frac{\partial \bar{Z}_{adv}}{\partial x} = -\frac{1}{2g} \frac{\partial \overline{U^2}}{\partial x}, \quad (9)$$

825 can be easily integrated to:

826
$$\bar{Z}_{adv} = -\frac{1}{2g} \left(\overline{U^2} - \overline{U_0^2} \right) = -\frac{1}{2} Fr_0^2 \left(\frac{\overline{U^2}}{\overline{U_0^2}} - 1 \right) \bar{h}_0 \quad (10)$$

827 where the Froude number is introduced, $\overline{Fr^2} = \overline{U^2}/(g\bar{h})$, which is computed with

设置了格式: 字体: (默认) Times New Roman
 设置了格式: 字体: (默认) Times New Roman
 设置了格式: 字体: (默认) Times New Roman
 设置了格式: 字体: (默认) Times New Roman
 域代码已更改

设置了格式: 字体: (默认) Times New Roman, 字体颜色: 文字 1
 设置了格式: 字体颜色: 文字 1, 检查拼写和语法
 设置了格式: 字体: (默认) Times New Roman, 字体颜色: 文字 1

828 the averaged variables. In this case, the correction is local (not cumulative) and
 829 proportional to the flow depth through a coefficient that is negligible as long as the
 830 velocity does not change significantly, and Fr is small, as is common in most tidal
 831 flows. It was shown by Savenije (2005, 2012) that the density term in equation (1)(+) ~~(1)~~
 832 always exercises a pressure in the landward direction, which is counteracted by a
 833 residual water level slope, amounting to 1.25% of the estuary depth over the salt
 834 intrusion length. The value for the residual water level slope, induced by the density
 835 effect, is usually small compared with the gradient of the free surface elevation; thus,
 836 in this paper, we neglect the influence of the density difference on the dynamics of the
 837 residual water level.

838

839 **Appendix B. Governing equations for tide-river dynamics in estuaries**

840 The analytical solutions for the dependent parameters μ , δ , λ , and ε are obtained by
 841 solving the following four dimensionless equations (see details in Cai et al., 2014a):
 842 the tidal damping/amplification equation, describing the tidal amplification or
 843 damping as a result of the balance between channel convergence (gq) and bottom
 844 friction (cm/G):

$$845 \quad \delta = \frac{\mu^2 (\gamma\theta - \chi\mu\lambda\Gamma)}{1 + \mu^2\beta}, \quad (911)$$

846 the scaling equation, describing how the ratio of velocity amplitude to tidal amplitude
 847 depends on phase lag and wave celerity:

$$848 \quad \mu = \frac{\sin(\varepsilon)}{\lambda} = \frac{\cos(\varepsilon)}{\gamma - \delta}, \quad (1012)$$

849 the celerity equation, describing how the wave celerity depends on the balance

850 between convergence and tidal damping/amplification:

851
$$\lambda^2 = 1 - \delta(\gamma - \delta), \quad (4413)$$

852 and the phase lag equation, describing how the phase lag between HW and HWS

853 depends on wave celerity, convergence, and damping:

854
$$\tan(\varepsilon) = \frac{\lambda}{\gamma - \delta}, \quad (4414)$$

855 where q , b , and G account for the effect of river discharge and where:

856
$$\beta = \theta - r_s \zeta \varphi / (\mu \lambda), \quad \theta = 1 - (\sqrt{1 + \zeta} - 1) \varphi / (\mu \lambda), \quad \Gamma = \frac{1}{\pi} [p_1 - 2p_2 \varphi + p_3 \varphi^2 (3 + \mu^2 \lambda^2 / \varphi^2)].$$

857
$$(4415)$$

858 Note that Γ is a friction factor obtained by using Chebyshev polynomials (Dronkers,

859 1964) to represent the non-linear friction term in the momentum equation:

860
$$F = \frac{U |U|}{K^2 h^{-4/3}} \approx \frac{1}{K^2 h^{-4/3} \pi} (p_0 v^2 + p_1 v U + p_2 U^2 + p_3 U^3 / v), \quad (4416)$$

861 in which U is the cross-sectional averaged velocity consisting of a steady component

862 U_r , generated by the fresh water discharge, and a time-dependent component U_t ,

863 introduced by the tide:

864
$$U = U_t - U_r = v \sin(\omega t) - Q / \bar{A}, \quad (4417)$$

865 where Q is the fresh water discharge (treated as a constant during the tidal wave

866 propagation), and p_i ($i = 0, 1, 2, 3$) are the Chebyshev coefficients (see Dronkers,

867 1964, p. 301), which are functions of the dimensionless river discharge φ through

868 $\alpha = \arccos(-\varphi)$:

869
$$p_0 = -\frac{7}{120} \sin(2\alpha) + \frac{1}{24} \sin(6\alpha) - \frac{1}{60} \sin(8\alpha), \quad (4418)$$

870
$$p_1 = \frac{7}{6} \sin(\alpha) - \frac{7}{30} (3\alpha) - \frac{7}{30} \sin(5\alpha) + \frac{1}{10} \sin(7\alpha), \quad (4419)$$

871
$$p_2 = \pi - 2\alpha + \frac{1}{3} \sin(2\alpha) + \frac{19}{30} \sin(4\alpha) - \frac{1}{5} \sin(6\alpha), \quad (4420)$$

872
$$p_3 = \frac{4}{3}\sin(\alpha) - \frac{2}{3}\sin(3\alpha) + \frac{2}{15}\sin(5\alpha). \quad (4921)$$

873 The coefficients p_1 , p_2 , and p_3 determine the magnitudes of the linear, quadratic, and
874 cubic frictional interaction, respectively.

875